Drell-Yan cross section in TMD factorisation

Valerio Bertone

Contents

1 Structure of the observables

Let us start from Eq. (2.6) of Ref. [1], that is the fully differential cross section for lepton-pair production in the region in which the TMD factorisation applies, *i.e.* $q_T \ll Q$. After some minor manipulations, it reads:

$$\frac{d\sigma}{dQdydq_T} = \frac{16\pi\alpha^2 q_T}{9Q^3} H(Q,\mu) \sum_q C_q(Q) \int \frac{d^2\mathbf{b}}{4\pi} e^{i\mathbf{b}\cdot\mathbf{q}_T} \overline{F}_q(x_1,\mathbf{b};\mu,\zeta)\overline{F}_{\bar{q}}(x_2,\mathbf{b};\mu,\zeta)\,, \tag{1.1}$$

where Q, y, and q_T are the invariant mass, the rapidity, and the transverse momentum of the lepton pair, respectively, while α is the electromagnetic coupling, H is the appropriate QCD hard factor that can be perturbatively computed, and C_q are the effective electroweak charges. In addition, the variables x_1 and x_2 are functions of Q and y and are given by:

$$x_{1,2} = \frac{Q}{\sqrt{s}}e^{\pm y}\,, \tag{1.2}$$

being $\sqrt{s}$ the centre-of-mass energy of the collision. In Eq. (1.1) we are using the short-hand notation:

$$\overline{F}_q(x,\mathbf{b};\mu,\zeta) \equiv xF_q(x,\mathbf{b};\mu,\zeta)\,, \tag{1.3}$$

that is convenient for the implementation. The scales μ and ζ are introduced as a consequence of the removal of UV and rapidity divergences in the definition of the TMDs. Despite these scales are arbitrary scales, they are typically chosen $\mu = \sqrt{\zeta} = Q$. Therefore, for all practical purposes their presence is fictitious.

The computation-intensive part of Eq.(1.1) has the form of the integral:

$$I_{ij}(x_1,x_2,q_T;\mu,\zeta) = \int \frac{d^2\mathbf{b}}{4\pi} e^{i\mathbf{b}\cdot\mathbf{q}_T} \overline{F}_i(x_1,\mathbf{b};\mu,\zeta)\overline{F}_j(x_2,\mathbf{b};\mu,\zeta)\,. \tag{1.4}$$

where $\overline{F}_{i(j)}$ are combinations of evolved TMD PDFs. At this stage, for convenience, i and j do not coincide with q and $\bar{q}$ but they are linked through a simple linear transformation. The integral over the bidimensional impact parameter $\mathbf{b}$ has to be taken. However, $\overline{F}_{i(j)}$ only depend on the absolute value of $\mathbf{b}$, therefore Eq. (1.4) can be written as:

$$I_{ij}(x_1, x_2, q_T; \mu, \zeta) = \frac{1}{2} \int_0^\infty db \, b J_0(bq_T) \overline{F}_i(x_1, b; \mu, \zeta) \overline{F}_j(x_2, b; \mu, \zeta) \,. \tag{1.5}$$

where J_0 is the zero-th order Bessel function of the first kind whose integral representation is:

$$J_0(x) = \frac{1}{2\pi} \int_0^{2\pi} d\theta e^{ix\cos(\theta)} \,. \tag{1.6}$$

The evolved quark TMD PDF $\overline{F}_i$ at the final scales μ and ζ is obtained by multiplying the same distribution at the initial scales μ_0 and ζ_0 by a single evolution factor R_q([1]). that is:

$$\overline{F}_i(x, b; \mu, \zeta) = R_q(\mu_0, \zeta_0 \to \mu, \zeta; b) \overline{F}_i(x, b; \mu_0, \zeta_0) \,. \tag{1.7}$$

The initial scale TMD PDFs at small values b can be written as:

$$\overline{F}_i(x, b; \mu_0, \zeta_0) = \sum_{j=g,q(\bar{q})} x \int_x^1 \frac{dy}{y} C_{ij}(y; \mu_0, \zeta_0) f_j\left(\frac{x}{y}, \mu_0\right) \,, \tag{1.8}$$

where f_j are the collinear PDFs (including the gluon) and C_{ij} are the so-called matching functions that are perturbatively computable and are currently known to NNLO, i.e. $\mathcal{O}(\alpha_s^2)$. If we define:

$$\overline{f}_i(x, \mu_0) = x f_i(x, \mu_0) \,, \tag{1.9}$$

Eq. (1.8) can be written as:

$$\overline{F}_i(x, b; \mu_0, \zeta_0) = \sum_{j=g,q(\bar{q})} \int_x^1 dy \, C_{ij}(y; \mu_0, \zeta_0) \overline{f}_i\left(\frac{x}{y}, \mu_0\right) \,. \tag{1.10}$$

Putting Eqs. (1.7) and (1.10), one finds:

$$\overline{F}_i(x, b; \mu, \zeta) = R_q(\mu_0, \zeta_0 \to \mu, \zeta; b) \sum_{j=g,q(\bar{q})} \int_x^1 dy \, C_{ij}(y; \mu_0, \zeta_0) \overline{f}_i\left(\frac{x}{y}, \mu_0\right) \,. \tag{1.11}$$

Matching and evolution are affected by non-perturbative effects that become relevant at large b. In order to account for such effects, one usually introduces a phenomenological function f_{NP}. In the traditional approach (CSS [2]), the b-space TMDs get a multiplicative correction that does not depend on the flavour. In addition, the perturbative content of the TMDs is smoothly damped away at large b by introducing the so-called b_*-prescription:

$$\overline{F}_i(x, b; \mu, \zeta) \to \overline{F}_i(x, b_*(b); \mu, \zeta) f_{\mathrm{NP}}(x, b, \zeta) \,, \tag{1.12}$$

where $b_* \equiv b_*(b)$ is a monotonic function of the impact parameter b such that:

$$\lim_{b \to 0} b_*(b) = b_{\min} \quad \text{and} \quad \lim_{b \to \infty} b_*(b) = b_{\max} \,, \tag{1.13}$$

being $b_{\min}$ and $b_{\max}$ constant values both in the perturbative region. Including the non-perturbative function, Eq. (1.5) becomes:

$$I_{ij}(x_1, x_2, q_T; \mu, \zeta) = \int_0^\infty db \, J_0(bq_T) \left[\frac{b}{2} \overline{F}_i(x_1, b_*(b); \mu, \zeta) \overline{F}_j(x_2, b_*(b); \mu, \zeta) f_{\mathrm{NP}}(x_1, b, \zeta) f_{\mathrm{NP}}(x_2, b, \zeta) \right]$$

$$= \frac{1}{q_T} \int_0^\infty d\bar{b} \, J_0(\bar{b}) \left[\frac{\bar{b}}{2q_T} \overline{F}_i\left(x_1, b_*\left(\frac{\bar{b}}{q_T}\right); \mu, \zeta\right) \overline{F}_j\left(x_2, b_*\left(\frac{\bar{b}}{q_T}\right); \mu, \zeta\right) f_{\mathrm{NP}}\left(x_1, \frac{\bar{b}}{q_T}, \zeta\right) f_{\mathrm{NP}}\left(x_2, \frac{\bar{b}}{q_T}, \zeta\right) \right] \,. \tag{1.14}$$

---

[1] Note that in Eq. (1.1) the gluon TMD PDF $\overline{F}_g$ is not involved. If also the gluon TMD PDF was involved, it would evolve by means of a different evolution factor R_g.

Eq. (1.14) is a Hankel tranform and can be efficiently computed using the so-called Ogata quadrature [3]. Effectively, the computation of the integral in Eq. (1.4) is achieved through a weighted sum:

$$I_{ij}(x_1, x_2, q_T; \mu, \zeta) \quad \simeq \quad \frac{1}{q_T} \sum_{n=1}^{N} \frac{w_n^{(0)} z_n^{(0)}}{2q_T} \overline{F}_i\left(x_1, b_*\left(\frac{z_n^{(0)}}{q_T}\right); \mu, \zeta\right) \overline{F}_j\left(x_2, b_*\left(\frac{z_n^{(0)}}{q_T}\right); \mu, \zeta\right)$$

$$\times \quad f_{\rm NP}\left(x_1, \frac{z_n^{(0)}}{q_T}, \zeta\right) f_{\rm NP}\left(x_2, \frac{z_n^{(0)}}{q_T}, \zeta\right),$$

(1.15)

where the unscaled coordinates $z_n^{(0)}$ and the weights $w_n^{(0)}$ can be precomputed in terms of the zero's of the Bessel function J_0 and one single parameter (see Ref. [3] for more details, specifically Eqs. (5.1) and (5.2) or Appendix A for the relevant formula to compute the unscaled coordinates and the weights)[2]. Based on the (empirically verified) assumption that the absolute value of each term in the sum in the r.h.s. of Eq. (1.15) is smaller than that of the preceding one, the truncation number N is chosen dynamically in such a way that the $(N+1)$-th term is smaller in absolute value than a user-defined cutoff relatively to the sum of the preceding N terms.

Eq. (1.15) factors out the non-perturbative part of the calculation represented by $f_{\rm NP}$ from the perturbative content. This is done on purpose to devise a method in which the perturbative content is precomputed and numerically convoluted with the non-perturbative functions *a posteriori*. This is convenient in view of a fit of the function $f_{\rm NP}$.

As customary in QCD, the most convenient basis for the matching in Eq. (1.8) is the so-called "evolution" basis (*i.e.* Σ, V, T_3, V_3, etc.). In fact, in this basis the operator matrix C_{ij} is almost diagonal with the only exception of crossing terms that couple the gluon and the singlet Σ distributions. As a consequence, this is the most convenient basis for the computation of I_{ij}. On the other hand, TMDs in Eq. (1.1) appear in the so-called "physical" basis (*i.e.* d, $\bar{d}$, u, $\bar{u}$, etc.). Therefore, we need to rotate $F_{i(j)}$ from the evolution basis, over which the indices i and j run, to the physical basis. This is done by means of an appropriate constant matrix T, so that:

$$\overline{F}_q(x_1, b; \mu, \zeta) = \sum_i T_{qi} F_i(x_1, b; \mu, \zeta),$$

(1.16)

and similarly for $\overline{F}_{\bar{q}}$. Putting all pieces together, one can conveniently write the cross section in Eq. (1.1) as:

$$\frac{d\sigma}{dQ dy dq_T} \simeq \sum_{n=1}^{N} w_n^{(0)} \frac{z_n^{(0)}}{q_T} S\left(x_1, x_2, \frac{z_n^{(0)}}{q_T}; \mu, \zeta\right) f_{\rm NP}\left(x_1, \frac{z_n^{(0)}}{q_T}, \zeta\right) f_{\rm NP}\left(x_2, \frac{z_n^{(0)}}{q_T}, \zeta\right),$$

(1.17)

with:

$$S(x_1, x_2, b; \mu, \zeta) = \frac{8\pi\alpha^2}{9Q^3} H(Q, \mu) \sum_q C_q(Q) \left[\overline{F}_q\left(x_1, b_*(b); \mu, \zeta\right)\right] \left[\overline{F}_{\bar{q}}\left(x_2, b_*(b); \mu, \zeta\right)\right].$$

(1.18)

Eq. (1.17) allows one to precompute the weights S in such a way that the differential cross section in Eq. (1.1) can be computed as a simple weighted sum of the non-perturbative contribution. A misleading aspect of Eq. (1.18) is the fact that S has five arguments. In actual facts, S only depends on three independent variables. The reason is that μ and ζ are usually taken to be proportional to Q by a constant factor. In addition x_1 and x_2 depend on Q and y through Eq. (1.2). Therefore, the full dependence on the kinematics of the final state of Eq. (1.1) can be specified by Q, y and q_T.

2 Integrating over the final-state kinematic variables

Despite Eq. (1.17) provides a powerful tool for a fast computation of cross sections, it is often not sufficient to allow for a direct comparison to experimental data. The reason is that experimental measurements of differential distributions are usually delivered as integrated over finite regions of the final-state kinematic phase space. In other words, experiments measure quantities like:

$$\widetilde{\sigma} = \int_{Q_{\min}}^{Q_{\max}} dQ \int_{y_{\min}}^{y_{\max}} dy \int_{q_{T,\min}}^{q_{T,\max}} dq_T \left[\frac{d\sigma}{dQ dy dq_T}\right].$$

(2.1)

---

[2] The superscript 0 in $z_n^{(0)}$ and $w_n^{(0)}$ indicates that here we are performing a Hankel tranform that involves the Bessel function of degree zero J_0. This is useful in view of the next section in which the integration over q_T will give rise to a similar Hankel transform with J_0 replaced by J_1. Also in that case the Ogata quadrature algorithm can be applied but coordinates and weights will be different.

As a consequence, in order to guarantee performance, we need to include the integrations above in the precomputed factors.

2.1 Integrating over q_T

The integration over bins in q_T can be carried out analytically exploiting the following property of Bessel's function:

$$\frac{d}{dx}\left[x^m J_m(x)\right] = x^m J_{m-1}(x)\,, \tag{2.2}$$

that leads to:

$$\int dx\, x J_0(x) = x J_1(x) \quad \Rightarrow \quad \int_{x_1}^{x_2} dx\, x J_0(x) = x_2 J_1(x_2) - x_1 J_1(x_1)\,. \tag{2.3}$$

To see it, we observe that the differential cross section in Eq. (1.1) has the following structure:

$$\frac{d\sigma}{dQ dy dq_T} \propto \int_0^\infty db\, q_T J_0(b q_T) \ldots \tag{2.4}$$

where the ellipses indicate terms that do not depend on q_T. Therefore, using Eq. (2.3) we find:

$$\int_{q_{T,\min}}^{q_{T,\max}} dq_T \left[\frac{d\sigma}{dQ dy dq_T}\right] \propto \int_0^\infty db \int_{q_{T,\min}}^{q_{T,\max}} dq_T\, q_T J_0(b q_T) \cdots =$$

$$\int_0^\infty \frac{db}{b^2} \int_{b q_{T,\min}}^{b q_{T,\max}} dx\, x J_0(x) \cdots = \int_0^\infty \frac{db}{b} \left[q_{T,\max} J_1(b q_{T,\max}) - q_{T,\min} J_1(b q_{T,\min})\right] \ldots\,. \tag{2.5}$$

Therefore, defining:

$$K(q_T) \equiv \int dq_T \left[\frac{d\sigma}{dQ dy dq_T}\right] \tag{2.6}$$

as the indefinite integral over q_T of the cross section in Eq. (1.1), we have that:

$$\int_{q_{T,\min}}^{q_{T,\max}} dq_T \left[\frac{d\sigma}{dQ dy dq_T}\right] = K(Q, y, q_{T,\max}) - K(Q, y, q_{T,\min})\,, \tag{2.7}$$

with:

$$K(Q, y, q_T) = \frac{8\pi\alpha^2 q_T}{9Q^3} H(Q, \mu)$$

$$\times \int_0^\infty db\, J_1(b q_T) \sum_q C_q(Q) \overline{F}_q(x_1, b; \mu, \zeta) \overline{F}_{\bar{q}}(x_2, b; \mu, \zeta) f_{\rm NP}(x_1, b, \zeta) f_{\rm NP}(x_2, b, \zeta)\,, \tag{2.8}$$

that can be computed using the Ogata quadrature as:

$$K(Q, y, q_T) \simeq \sum_{n=1}^N w_n^{(1)} S\left(x_1, x_2, \frac{z_n^{(1)}}{q_T}; \mu, \zeta\right) f_{\rm NP}\left(x_1, \frac{z_n^{(1)}}{q_T}, \zeta\right) f_{\rm NP}\left(x_2, \frac{z_n^{(1)}}{q_T}, \zeta\right)\,, \tag{2.9}$$

with S defined in Eq. (1.18). The unscaled coordinates $z_n^{(1)}$ and the weights $w_n^{(1)}$ can again be precomputed and stored in terms of the zero's of the Bessel function J_1. Eq. (2.7) reduces the integration in q_T to a calculation completely analogous to the unintegrated cross section. This is particularly convenient because it avoids the computation a numerical integration.

2.1.1 Kinematic cuts

In the presence of kinematic cuts, such as those on the final-state leptons in Drell-Yan, the analytic integration over q_T discussed above cannot be performed. The reason is that the implementation of these cuts effectively introduces a q_T-dependent function $\mathcal{P}(^3)$ in the integral:

$$\frac{d\sigma}{dQ dy dq_T} \propto \int_0^\infty db\, q_T J_0(b q_T) \mathcal{P}(q_T) \ldots\,, \tag{2.10}$$

---

[3] In fact, $\mathcal{P}$ also depends on the invariant mass Q and the rapidity y of the lepton pair that also need to be integrated over.

that prevents the direct use of Eq. (2.3). Since $\mathcal{P}$ is a slowly-varying function of q_T over the typical bin size, we can approximate the integral over the bins in q_T as:

$$\int_{q_{T,\min}}^{q_{T,\max}} dq_T \, q_T \, J_0(bq_T) \mathcal{P}(q_T) \quad \simeq \quad \mathcal{P}\left(\frac{q_{T,\max} + q_{T,\min}}{2}\right) \int_{q_{T,\min}}^{q_{T,\max}} dq_T \, q_T \, J_0(bq_T)$$

$$= \quad \mathcal{P}\left(\frac{q_{T,\max} + q_{T,\min}}{2}\right) \frac{1}{b} \left[q_{T,\max} J_1(bq_{T,\max}) - q_{T,\min} J_1(bq_{T,\min})\right] .$$

(2.11)

Unfortunately, this structure is inconvenient because it mixes different bin bounds and prevents a recursive computation. However, we can try to go further and, assuming that the bin width is small enough, we can expand $\mathcal{P}$ is the following ways:

$$\mathcal{P}\left(\frac{q_{T,\max} + q_{T,\min}}{2}\right) = \mathcal{P}\left(q_{T,\min} + \Delta q_T\right) = \mathcal{P}\left(q_{T,\min}\right) + \mathcal{P}'\left(q_{T,\min}\right)\Delta q_T + \mathcal{O}\left(\Delta q_T^2\right) ,$$

$$\mathcal{P}\left(\frac{q_{T,\max} + q_{T,\min}}{2}\right) = \mathcal{P}\left(q_{T,\max} - \Delta q_T\right) = \mathcal{P}\left(q_{T,\max}\right) - \mathcal{P}'\left(q_{T,\max}\right)\Delta q_T + \mathcal{O}\left(\Delta q_T^2\right) ,$$

(2.12)

with:

$$\Delta q_T = \frac{q_{T,\max} - q_{T,\min}}{2} .$$

(2.13)

Therefore:

$$b \int_{q_{T,\min}}^{q_{T,\max}} dq_T \, q_T \, J_0(bq_T)\mathcal{P}(q_T) \quad \simeq \quad q_{T,\max} J_1(bq_{T,\max}) \left[\mathcal{P}\left(q_{T,\max}\right) - \mathcal{P}'\left(q_{T,\max}\right)\Delta q_T\right]$$

$$- \quad q_{T,\min} J_1(bq_{T,\min}) \left[\mathcal{P}\left(q_{T,\min}\right) + \mathcal{P}'\left(q_{T,\min}\right)\Delta q_T\right] .$$

(2.14)

The advantage of this formula as compared to Eq. (2.11) is that each single term depends on one single bin-bound in q_T rather than on a combination of two consecutive bounds. Therefore, in the presence of kinematic cuts, the actual form of the primitive function K defined in Eq. (2.7) and given explicitly in Eq. (2.8) is:

$$K(Q, y, q_T) = \frac{8\pi\alpha^2 q_T}{9Q^3} H(Q, \mu) \left[\mathcal{P}\left(Q, y, q_T\right) \pm \mathcal{P}'\left(Q, y, q_T\right)\Delta q_T\right]$$

$$\times \int_0^\infty db \, J_1(bq_T) \sum_q C_q(Q) \overline{F}_q(x_1, b; \mu, \zeta) \overline{F}_{\bar{q}}(x_2, b; \mu, \zeta) f_{\rm NP}(x_1, b, \zeta) f_{\rm NP}(x_2, b, \zeta),$$

(2.15)

where I have explicitly reinstated the dependence of the function $\mathcal{P}$ and its derivative with respect to q_T, $\mathcal{P}'$, on Q and y. In the square bracket in Eq. (2.15), the minus sign applies when q_T is the upper bound of the bin and the plus sign when it is the lower bound (see Eq. (2.14)). As discussed below, when integrating over bins in Q and y, one should also integrate the functions $\mathcal{P}$ and $\mathcal{P}'$. However, we will argue that, in the interpolation procedure discussed below, these functions can be extracted from the integrals in Q and y in a proper manner in such a way to avoid computing the expensive function $\mathcal{P}$ many times and, moreover, simplify enormously the structure of the resulting interpolation tables.

2.2   On the position of the peak of the q_T distribution

It is interesting at this point to take a short detour to discuss the position of the peak on the distribution in q_T of the cross section in Eq. (1.1). The peak can be located by setting the derivative in q_T of the cross section equal to zero. To do so, we use another property of Bessel's functions:

$$\frac{dJ_0(x)}{dx} = -J_1(x) .$$

(2.16)

Using this relation, it is easy to see that:

$$0 = \frac{d}{dq_T}\left[\frac{d\sigma}{dQ\,dy\,dq_T}\right] =$$

$$\frac{8\pi\alpha^2}{9Q^3}H(Q,\mu)\int_0^\infty db\,b\,[J_0(bq_T)-bq_T J_1(bq_T)]\sum_q C_q(Q)\overline{F}_q(x_1,b_*(b);\mu,\zeta)\overline{F}_{\bar{q}}(x_2,b_*(b);\mu,\zeta) \tag{2.17}$$

$$\times f_{\rm NP}(x_1,b,\zeta)f_{\rm NP}(x_2,b,\zeta)\,,$$

that is equivalent to require that:

$$\int_0^\infty db\,b\,[J_0(bq_T)-bq_T J_1(bq_T)]\sum_q C_q(Q)\overline{F}_q(x_1,b_*(b);\mu,\zeta)\overline{F}_{\bar{q}}(x_2,b_*(b);\mu,\zeta)f_{\rm NP}(x_1,b,\zeta)f_{\rm NP}(x_2,b,\zeta) = 0\,. \tag{2.18}$$

The integral above can be solved numerically using the technique discussed above and the value of q_T that satisfies this equation represents the position of the peak of the q_T distribution.

2.3 Integrating over Q and y

As a final step, we need to perform the integrals over Q and y defined in Eq. (2.1). To compute these integrals we can only rely on numerical methods. Having reduced the integration in q_T to the difference of the two terms in the r.h.s. of Eq. (2.7)[4], we can concentrate on integrating the function K over Q and y for a fixed value of q_T:

$$\widetilde{K}(q_T) = \int_{Q_{\rm min}}^{Q_{\rm max}} dQ \int_{y_{\rm min}}^{y_{\rm max}} dy\,K(Q,y,q_T)\,, \tag{2.19}$$

such that:

$$\widetilde{\sigma} = \widetilde{K}(q_{T,\rm max}) - \widetilde{K}(q_{T,\rm min})\,. \tag{2.20}$$

To this purpose, it is convenient to make explicit the dependence of x_1 and x_2 on Q and y using Eq. (1.2). In addition, for the sake of simplicity we will identify the scales μ and $\sqrt{\zeta}$ with Q (possible scale variations can be easily reinstated at a later stage) and thus drop one of the arguments from the TMD distributions $\overline{F}$ and from the hard factor H. This yields:

$$\begin{aligned}\widetilde{K}(q_T) &= \frac{8\pi q_T}{9}\int_0^\infty db\,J_1(bq_T)\int_{Q_{\rm min}}^{Q_{\rm max}} dQ \int_{e^{y_{\rm min}}}^{e^{y_{\rm max}}} \frac{d\xi}{\xi} \\ &\quad \times \frac{1}{Q^3}\alpha^2(Q)H(Q)\sum_q C_q(Q)\overline{F}_q\left(\frac{Q}{\sqrt{s}}\xi,b_*(b);Q\right)\overline{F}_{\bar{q}}\left(\frac{Q}{\sqrt{s}}\frac{1}{\xi},b_*(b);Q\right) \\ &\quad \times f_{\rm NP}\left(\frac{Q}{\sqrt{s}}\xi,b;Q\right)f_{\rm NP}\left(\frac{Q}{\sqrt{s}}\frac{1}{\xi},b;Q\right)\,,\end{aligned} \tag{2.21}$$

where we have performed the change of variable $e^y = \xi$. Now we define one grid in ξ, $\{\xi_\alpha\}$ with $\alpha = 0,\ldots,N_\xi$, and one grid in Q, $\{Q_\tau\}$ with $\tau = 0,\ldots,N_Q$, each of which with a set of interpolating functions $\mathcal{I}$ associated. In addition, the grids are such that: $\xi_0 = e^{y_{\rm min}}$ and $\xi_{N_\xi} = e^{y_{\rm max}}$, and $Q_0 = Q_{\rm min}$ and $Q_{N_Q} = Q_{\rm max}$. This allows us to interpolate the pair of functions $f_{\rm NP}$ in Eq. (2.21) for generic values of ξ and Q as:

$$f_{\rm NP}\left(\frac{Q}{\sqrt{s}}\xi,b;Q\right)f_{\rm NP}\left(\frac{Q}{\sqrt{s}}\frac{1}{\xi},b;Q\right) \simeq \sum_{\alpha=0}^{N_\xi}\sum_{\tau=0}^{N_Q}\mathcal{I}_\alpha(\xi)\mathcal{I}_\tau(Q)f_{\rm NP}\left(\frac{Q_\tau}{\sqrt{s}}\xi_\alpha,b;Q_\tau\right)f_{\rm NP}\left(\frac{Q_\tau}{\sqrt{s}}\frac{1}{\xi_\alpha},b;Q_\tau\right)\,. \tag{2.22}$$

---

[4] For the moment we ignore the complication introduced by the presence of cuts on the final state discussed in Sect. 2.1.1. We will come back on this issue at the end of the section.

Plugging the equation above into Eq. (2.21) we obtain:

$$
\begin{aligned}
\widetilde{K}(q_T) \simeq & \frac{8\pi q_T}{9} \int_0^\infty db\, J_1(bq_T) \sum_{\tau=0}^{N_Q} \sum_{\alpha=0}^{N_\xi} \left[\int_{Q_{\min}}^{Q_{\max}} dQ\, \mathcal{I}_\tau(Q)\, \frac{1}{Q^3} \alpha^2(Q) H(Q) \right. \\
& \times \left. \int_{e^{y_{\min}}}^{e^{y_{\max}}} d\xi\, \mathcal{I}_\alpha(\xi)\, \frac{1}{\xi} \sum_q C_q(Q) \overline{F}_q\left(\frac{Q}{\sqrt{s}}\xi, b_*(b); Q\right) \overline{F}_{\bar{q}}\left(\frac{Q}{\sqrt{s}}\frac{1}{\xi}, b_*(b); Q\right) \right] \\
& \times f_{\rm NP}\left(\frac{Q_\tau}{\sqrt{s}}\xi_\alpha, b; Q_\tau\right) f_{\rm NP}\left(\frac{Q_\tau}{\sqrt{s}}\frac{1}{\xi_\alpha}, b; Q_\tau\right).
\end{aligned}
\tag{2.23}
$$

Finally, the integration over b can be performed using the Ogata quadrature as discussed above, so that:

$$
\begin{aligned}
\widetilde{K}(q_T) \simeq & \sum_{n=1}^N \sum_{\tau=0}^{N_Q} \sum_{\alpha=0}^{N_\xi} \left[\frac{8\pi}{9} w_n^{(1)} \int_{Q_{\min}}^{Q_{\max}} dQ\, \mathcal{I}_\tau(Q)\, \frac{1}{Q^3} \alpha^2(Q) H(Q) \right. \\
& \times \left. \int_{e^{y_{\min}}}^{e^{y_{\max}}} d\xi\, \mathcal{I}_\alpha(\xi)\, \frac{1}{\xi} \sum_q C_q(Q) \overline{F}_q\left(\frac{Q}{\sqrt{s}}\xi, b_*\left(\frac{z_n}{q_T}\right); Q\right) \overline{F}_{\bar{q}}\left(\frac{Q}{\sqrt{s}}\frac{1}{\xi}, b_*\left(\frac{z_n}{q_T}\right); Q\right) \right] \\
& \times f_{\rm NP}\left(\frac{Q_\tau}{\sqrt{s}}\xi_\alpha, \frac{z_n}{q_T}; Q_\tau\right) f_{\rm NP}\left(\frac{Q_\tau}{\sqrt{s}}\frac{1}{\xi_\alpha}, \frac{z_n}{q_T}; Q_\tau\right).
\end{aligned}
\tag{2.24}
$$

In conclusion, if we define:

$$
\begin{aligned}
W_{n\tau\alpha}(q_T) \equiv & w_n^{(1)} \frac{8\pi}{9} \int_{Q_{\min}}^{Q_{\max}} dQ\, \mathcal{I}_\tau(Q)\, \frac{\alpha^2(Q)}{Q^3} H(Q) \\
& \times \int_{e^{y_{\min}}}^{e^{y_{\max}}} d\xi\, \mathcal{I}_\alpha(\xi)\, \frac{1}{\xi} \sum_q C_q(Q) \overline{F}_q\left(\frac{Q}{\sqrt{s}}\xi, b_*\left(\frac{z_n}{q_T}\right); Q\right) \overline{F}_{\bar{q}}\left(\frac{Q}{\sqrt{s}}\frac{1}{\xi}, b_*\left(\frac{z_n}{q_T}\right); Q\right),
\end{aligned}
\tag{2.25}
$$

the quantity $\widetilde{K}(q_T)$ can be computed as:

$$
\widetilde{K}(q_T) \simeq \sum_{n=1}^N \sum_{\tau=0}^{N_Q} \sum_{\alpha=0}^{N_\xi} W_{n\tau\alpha}(q_T) f_{\rm NP}\left(\frac{Q_\tau}{\sqrt{s}}\xi_\alpha, \frac{z_n}{q_T}; Q_\tau\right) f_{\rm NP}\left(\frac{Q_\tau}{\sqrt{s}}\frac{1}{\xi_\alpha}, \frac{z_n}{q_T}; Q_\tau\right).
\tag{2.26}
$$

The advantage of Eq. (2.26) is that the weights $W_{n\alpha\tau}$, that clearly depend on q_T but also on the intervals $[Q_{\min} : Q_{\max}]$ and $[y_{\min} : y_{\max}]$, can be precomputed once and for all for each of the experimental points included in a fit and used to determine the function $f_{\rm NP}$. This provides a fast tool for the computation of predictions that makes the extraction of the non-perturbative part of the TMDs much easier.

It is now time to discuss how the weights defined in Eq. (2.25) are affected by the presence of cuts as discussed in Sect. 2.1.1. In principle, the function between square brackets in Eq. (2.15) should be inside the integrals in Eq. (2.25) and integrated over the variable Q and $\xi = e^y$. However, this turns out to be numerically problematic because the phase-space-reduction function $\mathcal{P}$ is expensive to compute. On top of this, the fact that the factor between square brackets in Eq. (2.15) depends on whether q_T is a lower or an upper integration bound would lead to a duplication of the weights to compute. In order to simplify the computation, we assume that the function $\mathcal{P}$ and its derivative $\mathcal{P}'$ are slowly varying functions of Q and y over the typical grid interval of the grids in Q and ξ. In addition, the interpolating functions $\mathcal{I}_\tau(Q)$ and $\mathcal{I}_\alpha(\xi)$ are strongly peaked at Q_τ and ξ_α, respectively. These considerations allow us to avoid integrating explicitly $\mathcal{P}$ and $\mathcal{P}'$ over Q and ξ and to replace the weights in Eq. (2.25) with:

$$
W_{n\tau\alpha}(q_T) \rightarrow \left[\mathcal{P}\left(Q_\tau, \ln(\xi_\alpha), q_T\right) \pm \mathcal{P}'\left(Q_\tau, \ln(\xi_\alpha), q_T\right) \Delta q_T \right] W_{n\tau\alpha}(q_T).
\tag{2.27}
$$

At the end of the day, the only additional information required to implement cuts on the final state is the value of the phase-space-reduction function $\mathcal{P}$ and its derivative $\mathcal{P}'$ on all points of the bidimensional grid in Q and ξ for all q_T bin bounds. Eq. (2.27) will then allow one to use the weights computed over the full phase space. We will check the accuracy of this procedure by comparing it to the explicit integration.

2.4   Cross section differential in x_F

In some cases, the Drell-Yan differential cross section may be presented as differential in the invariant mass of the lepton pair Q and, instead of the rapidity y, of the Feynman variable x_F defined as:

$$x_F = \frac{Q}{\sqrt{s}} \left(e^y - e^{-y} \right) = \frac{2Q}{\sqrt{s}} \sinh y = x_1 - x_2 \,, \tag{2.28}$$

so that:

$$\frac{dx_F}{dy} = \frac{2Q}{\sqrt{s}} \cosh y = x_1 + x_2 \,. \tag{2.29}$$

Therefore:

$$\frac{d\sigma}{dQ dx_F dq_T} = \frac{dy}{dx_F} \frac{d\sigma}{dQ dy dq_T} = \frac{\sqrt{s}}{2Q \cosh y} \frac{d\sigma}{dQ dy dq_T} = \frac{1}{x_1 + x_2} \frac{d\sigma}{dQ dy dq_T} \tag{2.30}$$

with:

$$y(x_F, Q) = \sinh^{-1} \left(\frac{x_F \sqrt{s}}{2Q} \right) = \ln \left[\frac{\sqrt{s}}{2Q} \left(x_F + \sqrt{x_F^2 + \frac{4Q^2}{s}} \right) \right] \,, \tag{2.31}$$

so that:

$$x_1 = \frac{1}{2} \left(x_F + \sqrt{x_F^2 + \frac{4Q^2}{s}} \right) \quad \text{and} \quad x_2 = \frac{Q^2}{s x_1} \,. \tag{2.32}$$

Therefore, we can compute the integral:

$$\widetilde{I}(q_T) = \int_{Q_{\min}}^{Q_{\max}} dQ \int_{x_{F,\min}}^{x_{F,\max}} dx_F \, I(Q, x_F, q_T) \,, \tag{2.33}$$

where I is the primitive in q_T of the cross section differential in x_F:

$$I(Q, x_F, q_T) = \int dq_T \left[\frac{d\sigma}{dQ dx_F dq_T} \right] \,, \tag{2.34}$$

following the same steps of Sect. 2.3. This leads to:

$$\widetilde{I}(q_T) \;\simeq\; \sum_{n=1}^{N} \sum_{\tau=0}^{N_Q} \sum_{\alpha=0}^{N_x} \overline{W}_{n\tau\alpha}(q_T) f_{\mathrm{NP}} \left(x_{1,\alpha\tau}, \frac{z_n}{q_T}; Q_\tau \right) f_{\mathrm{NP}} \left(x_{2,\alpha\tau}, \frac{z_n}{q_T}; Q_\tau \right) \,, \tag{2.35}$$

with:

$$\overline{W}_{n\tau\alpha}(q_T) \;\equiv\; w_n^{(1)} \frac{8\pi}{9} \int_{Q_{\min}}^{Q_{\max}} dQ \, \mathcal{I}_\tau(Q) \frac{1}{Q^3} \alpha^2(Q) H(Q)$$

$$\times \int_{x_{F,\min}}^{x_{F,\max}} dx_F \, \mathcal{I}_\alpha(x_F) \frac{1}{x_1 + x_2} \sum_q C_q(Q) \overline{F}_q \left(x_1, b_* \left(\frac{z_n}{q_T} \right); Q \right) \overline{F}_{\bar q} \left(x_2, b_* \left(\frac{z_n}{q_T} \right); Q \right) \,, \tag{2.36}$$

where x_1 and x_2 are functions of x_F and Q through Eq. (2.32). In addition, we have defined a grid in x_F, $\{x_{F,\alpha}\}$ with $\alpha = 0, \ldots, N_x$, that allowed us to define $x_{1(2),\alpha\tau} \equiv x_{1(2)}(x_{F,\alpha}, Q_\tau)$.

2.4.1   Approximated calculation of the cross section differential in x_F

In this section we explore the possibility of approximating the cross section differential in x_F and integrated over the bin in $x_F \in [x_{F,\min}, x_{F,\max}]$ in a way that the procedure developed in Sect. 2.3 can be used. The aim is to be able to compute predictions for the data delivered by the E772 experiment [4]. The specific observable measured in Ref. [4] is:

$$E \frac{d^3\sigma}{d^3q} = \frac{1}{2\pi q_T} \int_{Q_{\min}}^{Q_{\max}} dQ \frac{d\sigma}{dQ dy dq_T} \,, \tag{2.37}$$

where we have used the equality given in Eq. (43) of Ref. [5]. Integrating over the bin in x_F gives:

$$
\begin{aligned}
\int_{x_{F,\min}}^{x_{F,\max}} dx_F E \frac{d^3\sigma}{d^3q} &= \frac{1}{2\pi q_T} \int_{Q_{\min}}^{Q_{\max}} dQ \int_{x_{F,\min}}^{x_{F,\max}} dx_F \frac{d\sigma}{dQdydq_T} \\
&= \frac{1}{\pi q_T \sqrt{s}} \int_{Q_{\min}}^{Q_{\max}} dQ\, Q \int_{y(x_{F,\min},Q)}^{y(x_{F,\max},Q)} dy\, \cosh(y) \frac{d\sigma}{dQdydq_T} \,,
\end{aligned}
\tag{2.38}
$$

with $y(x_F,Q)$ given in Eq. (2.31). In order to reduce the leftmost integral to the structure of Eq. (2.19) where the integration bounds are constant, we assume that the bins in Q and x_F are small enough such that one can make the following approximation:

$$
\int_{x_{F,\min}}^{x_{F,\max}} dx_F E \frac{d^3\sigma}{d^3q} \simeq \frac{\overline{Q}\cosh(\overline{y})}{\pi q_T \sqrt{s}} \int_{Q_{\min}}^{Q_{\max}} dQ \int_{y(x_{F,\min},\overline{Q})}^{y(x_{F,\max},\overline{Q})} dy\, \frac{d\sigma}{dQdydq_T} \,,
\tag{2.39}
$$

where:

$$
\overline{Q} = \frac{Q_{\min} + Q_{\max}}{2} \quad \text{and} \quad \overline{y} = \frac{y(x_{F,\min},\overline{Q}) + y(x_{F,\max},\overline{Q})}{2} \,.
\tag{2.40}
$$

2.5   Flavour dependence

It may be advantageous to introduce a flavour dependence of the non-perturbative contributions to TMDs. This can be easily done by observing that the tensor $W_{n\tau\alpha}$ defined in Eq. (2.25) can be decomposed as[5]:

$$
W_{n\tau\alpha}(q_T) = \sum_q W_{n\tau\alpha}^{(q)}(q_T) \,,
\tag{2.41}
$$

with:

$$
\begin{aligned}
W_{n\tau\alpha}^{(q)}(q_T) &\equiv w_n^{(1)} \frac{8\pi}{9} \int_{Q_{\min}}^{Q_{\max}} dQ\, \mathcal{I}_\tau(Q) \frac{\alpha^2(Q)}{Q^3} H(Q) C_q(Q) \\
&\times \int_{e^{y_{\min}}}^{e^{y_{\max}}} d\xi\, \mathcal{I}_\alpha(\xi) \frac{1}{\xi} \overline{F}_q\left(\frac{Q}{\sqrt{s}}\xi, b_*\left(\frac{z_n}{q_T}\right); Q\right) \overline{F}_{\bar{q}}\left(\frac{Q}{\sqrt{s}}\frac{1}{\xi}, b_*\left(\frac{z_n}{q_T}\right); Q\right) \,.
\end{aligned}
\tag{2.42}
$$

This allows for an independent parameterisation of the non-perturbative contribution such that Eq. (2.26) can be written as:

$$
\widetilde{K}(q_T) \simeq \sum_q \sum_{n=1}^{N} \sum_{\tau=0}^{N_Q} \sum_{\alpha=0}^{N_\xi} W_{n\tau\alpha}^{(q)}(q_T) f_{\rm NP}^{(q)}\left(\frac{Q_\tau}{\sqrt{s}}\xi_\alpha, \frac{z_n}{q_T}; Q_\tau\right) f_{\rm NP}^{(q)}\left(\frac{Q_\tau}{\sqrt{s}}\frac{1}{\xi_\alpha}, \frac{z_n}{q_T}; Q_\tau\right) \,,
\tag{2.43}
$$

where $f_{\rm NP}^{(q)}$ parametrises the non-perturbative component of the TMD with flavour q.

2.6   Gradient with respect to the free parameters

A very appealing implication of the computation of cross section in terms of precomputed table as in Eqs. (2.26) and (2.43) is the fact that it exposes the free parameters of the non-perturbative functions. To be more specific, the non-perturbative function $f_{\rm NP}$, on top of being a function of x, b, and ζ, depends parameterically on a set of N_p parameters $\{\theta_k\}$, $k = 1, \ldots, N_p$, that are typically determined by fits to data, in other words:

$$
f_{\rm NP} \equiv f_{\rm NP}\left(x, b, \zeta; \{\theta_k\}\right) \,.
\tag{2.44}
$$

Now, when performing a fit, it is very useful to be able to compute the derivative of the figure of merit (usually the χ^2) with respect to the parameters to be determined. In turn, this immediately implies being able to compute the derivative of the observables. Referring to Eq. (2.26), the relevant quantity is:

$$
\frac{d\widetilde{K}}{d\theta_k} = \sum_{n=1}^{N} \sum_{\tau=0}^{N_Q} \sum_{\alpha=0}^{N_\xi} W_{n\tau\alpha}(q_T) \left[\frac{df_{\rm NP}^{(1)}}{d\theta_k} f_{\rm NP}^{(2)} + f_{\rm NP}^{(1)} \frac{df_{\rm NP}^{(2)}}{d\theta_k} \right] \,,
\tag{2.45}
$$

---

[5] The same procedure applies to the tensor $\overline{W}_{n\tau\alpha}$ defined in Eq. (2.36).

where $f_{\mathrm{NP}}^{(1)}$ and $f_{\mathrm{NP}}^{(2)}$ refer to the non-perturbative function f_{NP} computed in x_1 and x_2, respectively. It is thus clear that the derivatives w.r.t. the free parameters penetrates the observable. Since in most cases the derivative of f_{NP} can be computed analytically, this allows one to compute the gradient of the figure of merit analytically. This potentially makes any fit much simpler.

2.7 Narrow-width approximation

A possible alternative to the numerical integration in Q when the integration region includes the Z-peak region is the so-called narrow-width approximation (NWA). In the NWA one assumes that the width of the Z boson, Γ_Z, is much smaller than its mass, M_Z. This way one can approximate the peaked behaviour of the couplings $C_q(Q)$ around $Q = M_Z$ with a δ-function, *i.e.* $C_q(Q) \sim \delta(Q^2 - M_Z^2)$. Therefore, the integration over Q can be done analytically. The exact structure of the electroweak couplings is the following:

$$C_q(Q) = e_q^2 - 2e_q V_q V_e \chi_1(Q) + (V_e^2 + A_e^2)(V_q^2 + A_q^2)\chi_2(Q)\,, \tag{2.46}$$

with:

$$\begin{aligned} \chi_1(Q) &= \frac{1}{4\sin^2\theta_W \cos^2\theta_W} \frac{Q^2(Q^2 - M_Z^2)}{(Q^2 - M_Z^2)^2 + M_Z^2\Gamma_Z^2}\,, \\ \chi_2(Q) &= \frac{1}{16\sin^4\theta_W \cos^4\theta_W} \frac{Q^4}{(Q^2 - M_Z^2)^2 + M_Z^2\Gamma_Z^2}\,. \end{aligned} \tag{2.47}$$

In the limit $\Gamma_Z/M_Z \to 0$, the leading contribution to the coupling in Eq. (2.46) comes from the region $Q \simeq M_Z$ and is that proportional to χ_2:

$$C_q(Q) \simeq (V_e^2 + A_e^2)(V_q^2 + A_q^2)\chi_2(Q)\,, \quad Q \simeq M_Z\,. \tag{2.48}$$

In addition, in this limit one can show that:

$$\frac{1}{(Q^2 - M_Z^2)^2 + M_Z^2\Gamma_Z^2} \to \frac{\pi}{M_Z\Gamma_Z}\delta(Q^2 - M_Z^2) = \frac{\pi}{2M_Z^2\Gamma_Z}\delta(Q - M_Z)\,. \tag{2.49}$$

Therefore, considering that:

$$\Gamma_Z = \frac{\alpha M_Z}{\sin^2\theta_W \cos^2\theta_W}\,, \tag{2.50}$$

the electroweak couplings in the NWA have the following form:

$$C_q(Q) \simeq \frac{\pi M_Z(V_e^2 + A_e^2)(V_q^2 + A_q^2)}{32\alpha\sin^2\theta_W \cos^2\theta_W}\delta(Q - M_Z) = \widetilde{C}_q(Q)\delta(Q - M_Z)\,. \tag{2.51}$$

Therefore, using Eq. (2.48) the integral of the cross section over Q under the condition that $Q_{\min} < M_Z < Q_{\max}$ has the consequence of adjusting the couplings and of setting $Q = M_Z$ in the computation. This yields:

$$\int_{Q_{\min}}^{Q_{\max}} dQ\, \frac{d\sigma}{dQ\,dy\,dq_T} = \frac{16\pi\alpha^2 q_T}{9M_Z^3} H(M_Z, M_Z) \sum_q \widetilde{C}_q(M_Z) I_{q\bar{q}}(x_1, x_2, q_T; M_Z, M_Z^2)\,, \tag{2.52}$$

where we are also assuming that $\mu = \sqrt{\zeta} = M_Z$. As a final step, one may want to let the Z boson decay into leptons. At leading order in the EW sector and assuming an equal decay rate for electrons, muons, and tauons, this can be done by multiplying the cross section above by three times the branching ratio for the Z decaying into any pair of leptons, $3\mathrm{Br}(Z \to \ell^+\ell^-)$.

A   Ogata quadrature

In this section, we start by writing the formulas for the computation of the unscaled coordinates $z_n^{(\nu)}$ and weights $w_n^{(\nu)}$ required to compute the following integral:

$$\mathcal{I}_\nu(q_T) = \int_0^\infty db J_\nu(bq_T) f(b) = \frac{1}{q_T} \int_0^\infty d\bar{b} J_\nu(\bar{b}) f\left(\frac{\bar{b}}{q_T}\right) \simeq \frac{1}{q_T} \sum_{n=1}^\infty w_n^{(\nu)} f\left(\frac{z_n^{(\nu)}}{q_T}\right) \quad \nu = 0, 1, \dots, \quad (A.1)$$

using the Ogata-quadrature algorithm [3]. The relevant formulas are:

$$z_n^{(\nu)} = \frac{\pi}{h} \psi\left(\frac{h\xi_{\nu n}}{\pi}\right),$$

$$w_n^{(\nu)} = \pi \frac{Y_\nu(\xi_{\nu n})}{J_{\nu+1}(\xi_{\nu n})} J_\nu(z_n^{(\nu)}) \psi'\left(\frac{h\xi_{\nu n}}{\pi}\right).$$

$$(A.2)$$

where:

- h is a free parameter of the algorithm that has to be typically small (we choose $h = 10^{-3}$),

- $\xi_{\nu n}$ are the zero's of J_ν, i.e. $J_\nu(\xi_{\nu n}) = 0 \ \forall n$,

- J_ν and Y_ν are the Bessel functions of first and second kind, respectively, of degree ν,

- ψ is the following function:

$$\psi(t) = t \tanh\left(\frac{\pi}{2} \sinh t\right) \quad (A.3)$$

and its derivative:

$$\psi'(t) = \frac{\pi t \cosh t + \sinh(\pi \sinh t)}{1 + \cosh(\pi \sinh t)}. \quad (A.4)$$

We now move to rederive the formulas written above following (and to some extent simplifying) the main steps of Ref. [3] for the case $\nu = 0$ relevant to the computation of convolutions of unpolarised TMDs. The purpose is to eventually generalise the Ogata quadrature formula to a case in which more than a single Bessel function J_0 is present in the integrand.

As any other quadrature formula, also Ogata quadrature starts from interpolation. The starting point is the Lagrange interpolation formula over the grid $\xi_{-N}, \dots, \xi_{-1}, \xi_1, \dots, \xi_N$ for the function $f(x)$ that can be written as:

$$f(x) = \sum_{\substack{k=-N \\ k\neq 0}}^N f(\xi_k) \frac{W(x)}{W'(\xi_k)(x-\xi_k)}, \quad W(x) = \prod_{\substack{l=-N \\ l\neq 0}}^N \left(1 - \frac{x}{\xi_l}\right). \quad (A.5)$$

If we assume that $\xi_{-l} = -\xi_l$, we obtain:

$$W(x) = \prod_{l=1}^N \left(1 - \frac{x^2}{\xi_l^2}\right), \quad (A.6)$$

and if we also assume that $\{x_l\}$ are the (positive) zero's of J_0, i.e. $J_0(\xi_l) = 0$, we immediately obtain that $W(x) = J_0(x)$. Moreover, since $J_0'(x) = -J_1(x)$, we have that $W'(\xi_k) = -J_1(\xi_k)$ so that:

$$f(x) = -\sum_{\substack{k=-\infty \\ k\neq 0}}^\infty f(\xi_k) \frac{J_0(x)}{J_1(\xi_k)(x-\xi_k)}. \quad (A.7)$$

Now suppose we want to compute the integral:

$$\mathcal{I} = \int_{-\infty}^\infty dx |x| f(x) = -\sum_{\substack{k=-\infty \\ k\neq 0}}^\infty \frac{f(\xi_k)}{J_1(\xi_k)} \int_{-\infty}^\infty \frac{dx |x| J_0(x)}{x-\xi_k}. \quad (A.8)$$
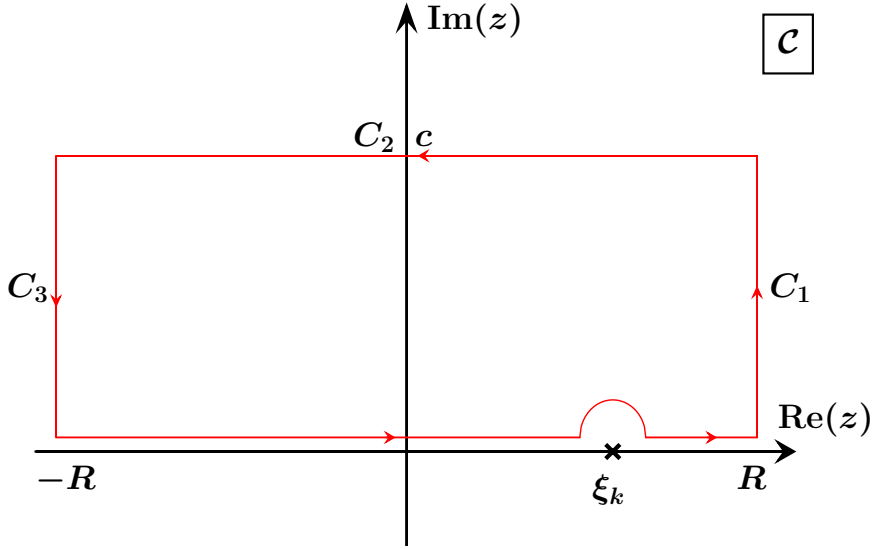
Fig. A.1: Integration contour $\mathcal{C}$ of Eq. (A.10).

Therefore, the task now boils down to computing:

$$\mathcal{J}_k = \int_{-\infty}^{\infty} \frac{dx\, |x| J_0(x)}{x - \xi_k} \,. \tag{A.9}$$

To do so, we consider the contour integral:

$$\int_{\mathcal{C}} \frac{dx\, |x| (J_0(x) + i Y_0(x))}{x - \xi_k} = 0 \,, \tag{A.10}$$

where $\mathcal{C}$ is the contour shown in Fig. A.1 and Y_0 is the Bessel function of the second kind. This integral vanishes because by construction the contour $\mathcal{C}$ contains no poles. One can show that, because of the specific combination $J_0(x) + i Y_0(x)$, the integrals along the paths C_1, C_2, and C_3 vanish as R and c tend to infinity. Moreover, the semi-circle around the pole at ξ_k tends to (minus) half the residue at ξ_k as the radius of the semi-circle tends to zero. One thus finds:

$$\int_{\mathcal{C}} \frac{dx\, |x| (J_0(x) + i Y_0(x))}{x - \xi_k} = \pi |\xi_k| Y_0(\xi_k) + \mathrm{PV} \int_{-\infty}^{\infty} \frac{dx\, |x| (J_0(x) + i Y_0(x))}{x - \xi_k} = 0 \,, \tag{A.11}$$

Since we are only interested in the real part of the last integral[6] and since the integrand of the real part is regular at $x = \xi_k$, we can get rid of the principal value prescription, thus obtaining:

$$\mathcal{J}_k = -\pi |\xi_k| Y_0(\xi_k) \,, \tag{A.12}$$

that finally produces:

$$\mathcal{I} = \sum_{\substack{k=-\infty \\ k \neq 0}}^{\infty} \frac{\pi Y_0(\xi_k)}{J_1(\xi_k)} |\xi_k| f(\xi_k) \,. \tag{A.13}$$

The integral in Eq. (A.14) can be rescaled by making a change of variable $x \to hx$ where h is a positive real number, so that:

$$\mathcal{I} = h \int_{-\infty}^{\infty} dx\, |hx| f(hx) = \pi h \sum_{\substack{k=-\infty \\ k \neq 0}}^{\infty} \frac{Y_0(\xi_k)}{J_1(\xi_k)} |h\xi_k| f(h\xi_k) \,, \tag{A.14}$$

which reproduces the result of Ref. [3] when $\nu = 0$.

---

[6] One should in principle prove that the imaginary part vanishes but, as in Ref. [3], we will not do it.
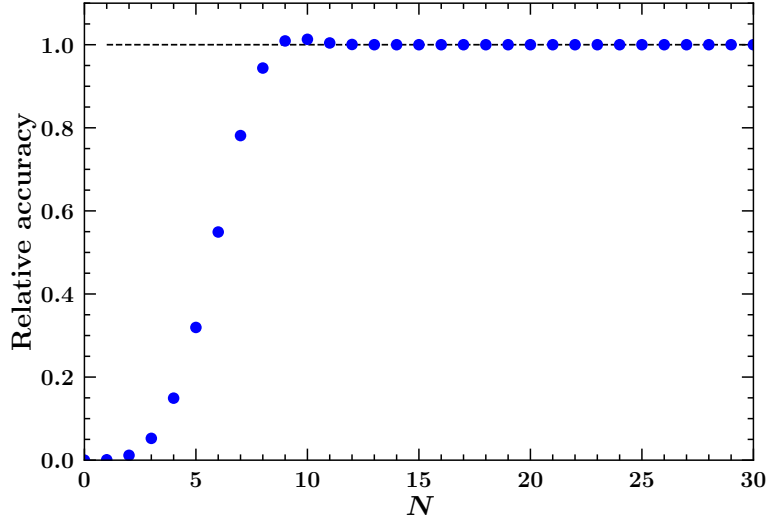
Fig. A.2: Relative accuracy of the integral in the l.h.s. of Eq. (A.19) computed by means of Eq. (A.17) truncated to the N-th term.

Now let us consider the specific integral in Eq. (A.1) with $\nu = 0$:

$$\mathcal{I}_0(q_T) = \frac{1}{q_T} \int_0^\infty d\bar{b} J_0(\bar{b}) f\left(\frac{\bar{b}}{q_T}\right) . \tag{A.15}$$

If we make the change of variable:

$$\bar{b} = \frac{\pi}{h} \psi\left(\frac{t}{\pi}\right) , \tag{A.16}$$

with ψ given in Eq. (A.3), we obtain:

$$\begin{aligned}
\mathcal{I}_0(q_T) &= \frac{1}{q_T} \frac{1}{h} \int_0^\infty dt\, \psi'\left(\frac{t}{\pi}\right) J_0\left(\frac{\pi}{h}\psi\left(\frac{t}{\pi}\right)\right) f\left(\frac{1}{q_T}\frac{\pi}{h}\psi\left(\frac{t}{\pi}\right)\right) \\
&= \frac{\pi}{q_T} \sum_{k=1}^\infty \frac{Y_0(\xi_k)}{J_1(\xi_k)} \psi'\left(\frac{h\xi_k}{\pi}\right) J_0\left(\frac{\pi}{h}\psi\left(\frac{h\xi_k}{\pi}\right)\right) f\left(\frac{1}{q_T}\frac{\pi}{h}\psi\left(\frac{h\xi_k}{\pi}\right)\right) ,
\end{aligned} \tag{A.17}$$

that finally agrees with Eq. (A.1). Note that, since the integral in between zero and infinity, we limited the series in k only to positive values. It is important to notice that the function ψ has been chosen such that:

$$\frac{\pi}{h} \psi\left(\frac{h\xi_k}{\pi}\right) \xrightarrow[k\to\infty]{} \xi_k , \tag{A.18}$$

so that the presence of J_0 suppresses contributions with large values of k thus allowing to truncate the series.

As an application of Eq. (A.17), we consider the integral:

$$\int_0^\infty db\, b J_0(b) e^{-\frac{b^2}{2}} = e^{-\frac{1}{2}} . \tag{A.19}$$

In Fig. A.2, the relative accuracy between the l.h.s. of Eq. (A.19) computed using Eq. (A.17) truncated to the N-th term and with $h = 10^{-3}$ and its true value given on the r.h.s. is plotted as a function of N. It is clear that the series quickly converges to its true value as N increases.

We now want to compute a generalisation of the integrals considered so far. Specifically:

$$\mathcal{K}_0(h_{0T}, h_{1T}, h_{2T}) = \int_0^\infty db\, b J_0(h_{T0}b) J_0(h_{1T}b) J_0(h_{2T}b) f(b) = \frac{1}{h_{T0}} \int_0^\infty d\bar{b}\, J_0(\bar{b}) J_0(a_1\bar{b}) J_0(a_2\bar{b}) f\left(\frac{\bar{b}}{h_{T0}}\right) , \tag{A.20}$$

where $a_i = h_{Ti}/h_{T0}$. The difference w.r.t. Eq. (A.1) is the fact that now the integrand contains three, rather than one, Bessel functions generally out of phase (*i.e.* $a_i \neq 1$). Integrals of this kind, that emerge when
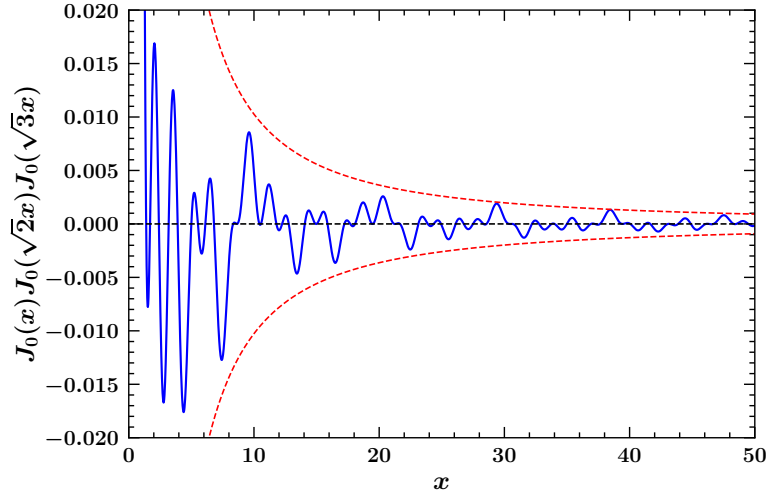
Fig. A.3: Behaviour of the product of three Bessel functions out of phase.

attempting to parameterise TMDs in transverse-momentum space rather than in impact-parameter space, are particularly nasty to evaluate numerically. Indeed, the combination of three Bessel functions out of phase gives rise to a highly "chaotic" oscillating behaviour that makes a brute-force computation very inefficient: Fig. (A.3) shows one such product.

Therefore, we need to develop an *ad hoc* quadrature method aimed at making the computation of the integral in Eq. (A.20) efficient. To do so, we follow the step taken by Ogata in Ref. [3] by generalising his arguments. As in that case, the starting formula to develop a quadrature integration is the Lagrange interpolation formula in Eq. (A.5), but this time the function W is the product of three Bessel functions rather than a single Bessel function. If for the moment we assume that $a_1, a_2, a_1/a_2 \neq 1$, we are guaranteed that there are no overlapping zero's of the three J_0, [7] we have that:

$$W(x) = J_0(x)J_0(a_1x)J_0(a_2x) = \prod_{l=1}^{\infty}\left(1 - \frac{x^2}{\overline{\xi}_l}\right), \tag{A.21}$$

where $\{\overline{\xi}_l\}$ is the union of the zero's of $J_0(x)$, $J_0(a_1x)$, and $J_0(a_2x)$ that, given the assumption above, never overlap. The computation of the derivative of W computed in the node $\overline{\xi}_k$ is easily computed:

$$W'(\overline{\xi}_k) = \begin{cases} -J_1(\overline{\xi}_k)J_0(a_1\overline{\xi}_k)J_0(a_2\overline{\xi}_k) & \overline{\xi}_k \text{ iz a zero of } J_0(x), \\ -a_1J_0(\overline{\xi}_k)J_1(a_1\overline{\xi}_k)J_0(a_2\overline{\xi}_k) & \overline{\xi}_k \text{ iz a zero of } J_0(a_1x), \\ -a_2J_0(\overline{\xi}_k)J_0(a_1\overline{\xi}_k)J_1(a_2\overline{\xi}_k) & \overline{\xi}_k \text{ iz a zero of } J_0(a_2x). \end{cases} \tag{A.22}$$

This allows us to write:

$$
\begin{aligned}
f(x) = & -\sum_{\overline{\xi}_k \in \{\xi_l\}} f(\overline{\xi}_k)\frac{J_0(x)J_0(a_1x)J_0(a_2x)}{J_1(\overline{\xi}_k)J_0(a_1\overline{\xi}_k)J_0(a_2\overline{\xi}_k)(x - \overline{\xi}_k)} \\
& -\sum_{\overline{\xi}_k \in \{\xi_l/a_1\}} f(\overline{\xi}_k)\frac{J_0(x)J_0(a_1x)J_0(a_2x)}{a_1J_0(\overline{\xi}_k)J_1(a_1\overline{\xi}_k)J_0(a_2\overline{\xi}_k)(x - \overline{\xi}_k)} \\
& -\sum_{\overline{\xi}_k \in \{\xi_l/a_2\}} f(\overline{\xi}_k)\frac{J_0(x)J_0(a_1x)J_0(a_2x)}{a_2J_0(\overline{\xi}_k)J_0(a_1\overline{\xi}_k)J_1(a_2\overline{\xi}_k)(x - \overline{\xi}_k)},
\end{aligned} \tag{A.23}
$$

---

[7] Actually, one should require that no zero's overlap, that amounts to requiring $a_1, a_2, a_1/a_2 \neq \xi_k/\xi_j$, $\forall i, j$. But configurations that violate this constraint are highly unlikely, except when $k = j$, that is when $a_1, a_2, a_1/a_2 = 1$.

where $\{\xi_l\}$ is the set of zero's of $J_0(x)$, that can be rewritten as:

$$
\begin{aligned}
f(x) \;=\; & -\sum_{\substack{k=-\infty \\ k\neq 0}}^{\infty} f(\xi_k)\frac{J_0(x)J_0(a_1x)J_0(a_2x)}{J_1(\xi_k)J_0(a_1\xi_k)J_0(a_2\xi_k)(x-\xi_k)} \\
& -\sum_{\substack{k=-\infty \\ k\neq 0}}^{\infty} f(\xi_k/a_1)\frac{J_0(x)J_0(a_1x)J_0(a_2x)}{a_1J_0(\xi_k/a_1)J_1(\xi_k)J_0(a_2\xi_k/a_1)(x-\xi_k/a_1)} \\
& -\sum_{\substack{k=-\infty \\ k\neq 0}}^{\infty} f(\xi_k/a_2)\frac{J_0(x)J_0(a_1x)J_0(a_2x)}{a_2J_0(\xi_k/a_2)J_0(a_1\xi_k/a_2)J_1(\xi_k)(x-\xi_k/a_2)}\,.
\end{aligned}
\tag{A.24}
$$

The resulting quadrature integral is:

$$
\begin{aligned}
\int_{-\infty}^{\infty} dx\,|x|f(x) \;=\; & -\sum_{\substack{k=-\infty \\ k\neq 0}}^{\infty} \frac{|\xi_k|f(\xi_k)}{J_1(\xi_k)J_0(a_1\xi_k)J_0(a_2\xi_k)}\frac{1}{\xi_k}\int_{-\infty}^{\infty}\frac{dy\,|y|J_0(a_1y)J_0(a_2y)J_0(y)}{y-\xi_k} \\
& -\sum_{\substack{k=-\infty \\ k\neq 0}}^{\infty} \frac{|\xi_k/a_1|f(\xi_k/a_1)}{a_1J_0(\xi_k/a_1)J_1(\xi_k)J_0(a_2\xi_k/a_1)}\frac{1}{\xi_k}\int_{-\infty}^{\infty}\frac{dy\,|y|J_0(y/a_1)J_0(a_2y/a_1)J_0(y)}{y-\xi_k} \\
& -\sum_{\substack{k=-\infty \\ k\neq 0}}^{\infty} \frac{|\xi_k/a_2|f(\xi_k/a_2)}{a_2J_0(\xi_k/a_2)J_0(a_1\xi_k/a_2)J_1(\xi_k)}\frac{1}{\xi_k}\int_{-\infty}^{\infty}\frac{dy\,|y|J_0(y/a_2)J_0(a_1y/a_2)J_0(y)}{y-\xi_k}\,.
\end{aligned}
\tag{A.25}
$$

Therefore, we need to compute integrals of the following kind:

$$
\mathcal{L}_k(c_1,c_2) = -\frac{1}{\xi_k}\int_{-\infty}^{\infty}\frac{dy\,|y|J_0(c_1y)J_0(c_2y)J_0(y)}{y-\xi_k}\,,
\tag{A.26}
$$

where c_1 and c_2 are such that $J_0(c_i\xi_k) \neq 0\ \forall k$. The solution proceeds similarly as above but we need to consider slightly more complicated contour integrals. In order to understand better the subtleties behind the computation of these integrals, we start from a case with two bessel functions:

$$
\int_{-\infty}^{\infty}\frac{dy\,|y|J_0(ay)J_0(by)}{y-t}\,,
\tag{A.27}
$$

where a and b are two positive numbers and t is a real number that does not need to be equal to a zero of $J_0(x)$. As above, we consider the contour integral:

$$
\int_{\mathcal{C}}\frac{dy\,|y|J_0(ay)H_0^{(1)}(by)}{y-t}\,,
\tag{A.28}
$$

where $H_0^{(1)}(y) = J_0(y) + iY_0(y)$ is the Hankel function and $\mathcal{C}$ is the same contour as in Fig. A.1. The subtlety here is to guarantee that the contribution from C_2 vanishes. To do so, we consider the asymptotic behavior of $H_0^{(1)}$ and J_0 for complex numbers with large absolute value. The relevant formulas here are:

$$
|H_0^{(1)}(z)| = \sqrt{\frac{2}{\pi|z|}}\exp(-\operatorname{Im}z)\left(1+\mathcal{O}(|z|^{-1})\right)\,,\quad 0\leq\arg z\leq\pi\,,
$$

$$
|J_0^{(1)}(z)| = \sqrt{\frac{2}{\pi|z|}}\left(\cos z + \exp(-\operatorname{Im}z)\mathcal{O}(|z|^{-1})\right) = \sqrt{\frac{1}{2\pi|z|}}\left(\exp(\operatorname{Im}z) + \exp(-\operatorname{Im}z)(1+\mathcal{O}(|z|^{-1}))\right)\,,\quad 0\leq\arg z\leq\pi\,.
\tag{A.29}
$$

In order for $|J_0(ay)||H_0^{(1)}(by)|$ to vanish as $\operatorname{Im}z$ gets large we need that $\exp((a-b)\operatorname{Im}z)$ is suppressed, which implies $a < b$. Under this condition, we can use the same method that we have used fot the single-Bessel case and obtain:

$$
0 = \int_{\mathcal{C}}\frac{dy\,|y|J_0(ay)H_0^{(1)}(by)}{y-t} = -i\pi|t|J_0(at)H_0^{(1)}(bt) + \mathrm{PV}\int_{-\infty}^{\infty}\frac{dy\,|y|J_0(ay)H_0^{(1)}(by)}{y-t}\,.
\tag{A.30}
$$

Now setting $b = 1$, so that $a < 1$, and $t = \xi_k$, and considering only the real part of the equality above, we obtain:

$$\int_{-\infty}^{\infty} \frac{dy\,|y|J_0(ay)J_0(y)}{y - \xi_k} = -\pi|\xi_k|J_0(a\xi_k)Y_0^{(1)}(\xi_k)\,, \quad a < 1\,. \tag{A.31}$$

If instead $a > b$, it is sufficient to exchange a and b in Eq. (A.30) which, setting $b = 1$ and $t = \xi_k$, produces:

$$\int_{-\infty}^{\infty} \frac{dy\,|y|J_0(ay)J_0(y)}{y - \xi_k} = 0\,, \quad a > 1\,. \tag{A.32}$$

The general result is thus:

$$\int_{-\infty}^{\infty} \frac{dy\,|y|J_0(ay)J_0(y)}{y - \xi_k} = -\theta(1 - a)\pi|\xi_k|J_0(a\xi_k)Y_0^{(1)}(\xi_k)\,. \tag{A.33}$$

We can now move to the three-Bessel case which implies considering the contour integral:

$$\int_{\mathcal{C}} \frac{dy\,|y|J_0(ay)J_0(by)H_0^{(1)}(cy)}{y - t}\,, \tag{A.34}$$

whose convergence requires that $a + b < c$. Under this assumption, one finds:

$$\mathrm{PV}\int_{-\infty}^{\infty} \frac{dy\,|y|J_0(ay)J_0(by)J_0(cy)}{y - t} = \mathrm{Re}\left[i\pi|t|J_0(at)J_0(bt)H_0^{(1)}(ct)\right]\,, \quad a + b < c\,. \tag{A.35}$$

However, other possible hierarchies can be accommodated by just reshuffling the arguments appropriately. There are two additional possibilities: $a + c < b$ and $b + c < a$, that produce the general result

$$\begin{aligned}
\mathrm{PV}\int_{-\infty}^{\infty} \frac{dy\,|y|J_0(ay)J_0(by)J_0(cy)}{y - t} &= \theta(c - a - b)\mathrm{Re}\left[i\pi|t|J_0(at)J_0(bt)H_0^{(1)}(ct)\right] \\
&+ \theta(b - a - c)\mathrm{Re}\left[i\pi|t|J_0(at)J_0(ct)H_0^{(1)}(bt)\right] \\
&+ \theta(a - b - c)\mathrm{Re}\left[i\pi|t|J_0(bt)J_0(ct)H_0^{(1)}(at)\right]\,.
\end{aligned} \tag{A.36}$$

Setting $a = c_1$, $b = c_2$, $c = 1$, and $t = \xi_k$, we obtain:

$$\mathcal{L}_k(c_1, c_2) = -\theta(1 - c_1 - c_2)\pi J_0(c_1\xi_k)J_0(c_2\xi_k)Y_0(\xi_k) + \theta(|c_1 - c_2| - 1) \times 0\,. \tag{A.37}$$

However, this is not the whole story because we still need to cover the region $c_1 + c_2 > 1$. Referring to Fig. A.4, the first term in the r.h.s. of Eq. (A.37) covers the red region while the second covers the blue regions. Therefore, we still need to cover the green region. Unfortunately, the computation in this region is particularly cumbersome. In order to make some steps forward, we first rewrite our target integral as follows:

$$\mathrm{PV}\int_{-\infty}^{\infty} \frac{dy\,|y|J_0(ay)J_0(by)J_0(cy)}{y - t} = 2t\,\mathrm{PV}\int_{0}^{\infty} \frac{dy\,yJ_0(ay)J_0(by)J_0(cy)}{y^2 - t^2}\,. \tag{A.38}$$

We now consider the contour integral:

$$\int_{\mathcal{P}} \frac{dy\,yH_0^{(1)}(ay)H_0^{(1)}(by)J_0(cy)}{y^2 - t^2} = 0\,, \tag{A.39}$$

where, assuming $t > 0$, $\mathcal{P}$ is the contour of the upper-right pizza slice with infinite radius and an infinitely small semi-circle around t removed (see Fig. A.5). Since this contour contains no poles the integral must evaluate to zero. However, In order for the integral along the quarter of circle at infinitt to give a vanishing contribution, we need to require $c - b - a <$. Under this requirement, we have:

$$\mathrm{PV}\int_{0}^{\infty} \frac{dy\,yH_0^{(1)}(ay)H_0^{(1)}(by)J_0(cy)}{y^2 - t^2} = \frac{i\pi}{2}H_0^{(1)}(at)H_0^{(1)}(bt)J_0(ct) - \frac{4}{\pi^2}\int_{0}^{\infty} \frac{dz\,zK_0(az)K_0(bz)I_0(cz)}{z^2 + t^2}\,, \tag{A.40}$$
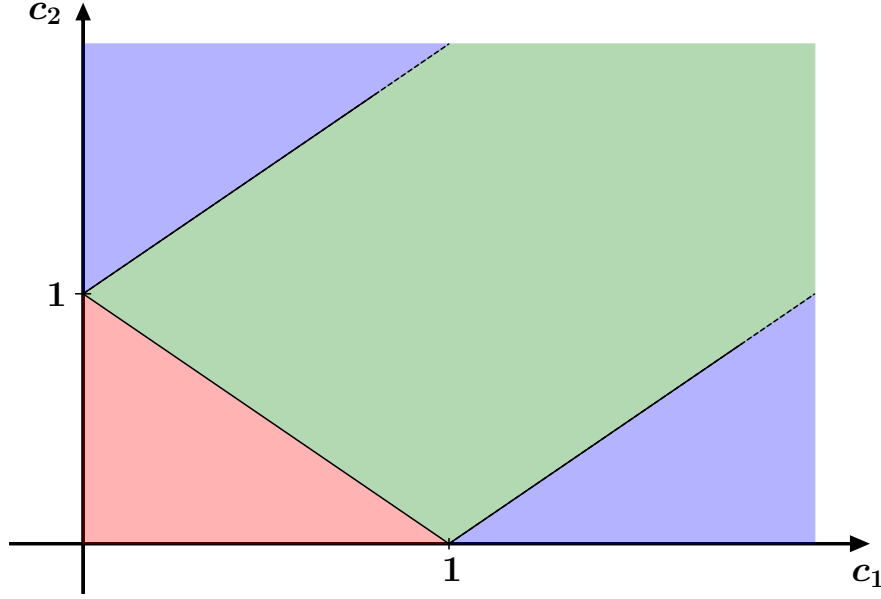
Fig. A.4: Domain of the interpolation weight $\mathcal{L}_k(c_1, c_2)$ in Eq. (A.26).

where we have used the identities $J_0(ix) = I_0(x)$ and $H_0^{(1)}(ix) = 2K_0(x)/(i\pi)$. If we focus on the real part of this equality and set $t = \xi_k$, we find:

$$\text{PV}\int_0^\infty \frac{dy\, y[J_0(ay)J_0(by) - Y_0(ay)Y_0(by)]J_0(cy)}{y^2 - \xi_k^2} = -\frac{4}{\pi^2}\int_0^\infty \frac{dz\, zK_0(az)K_0(bz)I_0(cz)}{z^2 + \xi_k^2}\,. \tag{A.41}$$

As above, we have three independent ways of matching a, b, and c with c_1, c_2, and 1. They are: 1) $a = c_1$, $b = c_2$, $c = 1$ valid for $c_2 > 1 - c_1$, 2) $a = 1$, $b = c_1$, $c = c_2$ valid for $c_2 < c_1 + 1$, 3) $a = c_2$, $b = 1$, $c = c_1$ valid for $c_2 > c_1 - 1$. Therefore, the overlap region of all three combinations is precisely the green region in Fig. A.4 that we are interested in. Assuming to concentrate on this region, we have:

$$\text{PV}\int_0^\infty \frac{dy\, y[J_0(c_1y)J_0(c_2y) - Y_0(c_1y)Y_0(c_2y)]J_0(y)}{y^2 - \xi_k^2} = -\frac{4}{\pi^2}\int_0^\infty \frac{dz\, zK_0(c_1z)K_0(c_2z)I_0(z)}{z^2 + \xi_k^2}\,,$$

$$\text{PV}\int_0^\infty \frac{dy\, y[J_0(y)J_0(c_1y) - Y_0(y)Y_0(c_1y)]J_0(c_2y)}{y^2 - \xi_k^2} = -\frac{\pi}{2}Y_0(\xi_k)J_0(c_1\xi_k)J_0(c_2\xi_k) - \frac{4}{\pi^2}\int_0^\infty \frac{dz\, zK_0(z)K_0(c_1z)I_0(c_2z)}{z^2 + \xi_k^2}\,,$$

$$\text{PV}\int_0^\infty \frac{dy\, y[J_0(c_2y)J_0(y) - Y_0(c_2y)Y_0(y)]J_0(c_1y)}{y^2 - \xi_k^2} = -\frac{\pi}{2}J_0(c_1\xi_k)Y_0(\xi_k)J_0(c_2\xi_k) - \frac{4}{\pi^2}\int_0^\infty \frac{dz\, zK_0(c_2z)K_0(z)I_0(c_1z)}{z^2 + \xi_k^2}\,. \tag{A.42}$$

All integrals above involve our target integral, *i.e.* the one with three J_0. However, this integral appears entangled with other integrals. In order to disentangle it, we consider the yet another vanishing integral:

$$\int_{\mathcal{P}} \frac{dy\, yH_0^{(1)}(ay)H_0^{(1)}(by)H_0^{(1)}(cy)}{y^2 - t^2} = 0\,, \tag{A.43}$$

where $\mathcal{P}$ is the contour in Fig. A.5. In this case, the quarter of circle at infinity gives a vanishing contribution for any value of a, b, and c, so that:

$$\text{PV}\int_0^\infty \frac{dy\, yH_0^{(1)}(ay)H_0^{(1)}(by)H_0^{(1)}(cy)}{y^2 - t^2} = \frac{i\pi}{2}H_0^{(1)}(at)H_0^{(1)}(bt)H_0^{(1)}(ct) + \frac{8i}{\pi^3}\int_0^\infty \frac{dz\, zK_0(az)K_0(bz)K_0(cz)}{z^2 + t^2}\,. \tag{A.44}$$

Setting as usual $t = \xi_k$, in this case there is only one independent way to matching a, b, and c with c_1, c_1 and
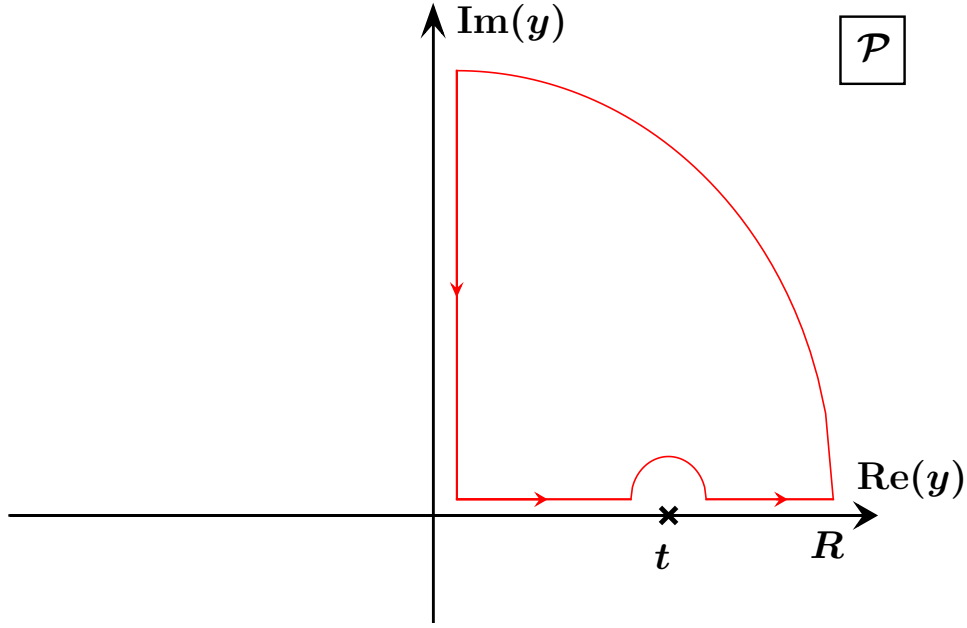
Fig. A.5: Integration contour $\mathcal{P}$ of Eq. (A.39).

1, and we choose it to be: $a = c_1$, $b = c_2$, and $c = 1$. Then we focus on the real part obtaining:

$$\text{PV} \int_0^\infty \frac{dy\, y[J_0(c_1 y)J_0(c_2 y)J_0(y) - Y_0(c_1 y)Y_0(c_2 y)J_0(y) - Y_0(y)Y_0(c_1 y)J_0(c_2 y) - Y_0(c_2 y)Y_0(y)J_0(c_1 y)]}{y^2 - \xi_k^2} =$$

$$-\frac{\pi}{2}[J_0(c_1\xi_k)J_0(c_2\xi_k) - Y_0(c_1\xi_k)Y_0(c_2\xi_k)]Y_0(\xi_k)\,.$$

(A.45)

Now we can sum all integrals in Eq. (A.42) and subtract off the integral in Eq. (A.45). This finally allows us to disentangle our target integral that yields:

$$\int_{-\infty}^\infty \frac{dy\, |y|J_0(c_1 y)J_0(c_2 y)J_0(y)}{y^2 - \xi_k^2} = -\frac{\pi}{2}|\xi_k|[J_0(c_1\xi_k)J_0(c_2\xi_k) + Y_0(c_1\xi_k)Y_0(c_2\xi_k)]Y_0(\xi_k)$$

$$- \frac{4}{\pi^2}|\xi_k| \int_0^\infty \frac{dz\, z[K_0(c_1 z)K_0(c_2 z)I_0(z) + K_0(z)K_0(c_1 z)I_0(c_2) + K_0(c_2 z)K_0(z)I_0(c_1 z)]}{z^2 + \xi_k^2}\,,$$

(A.46)

valid for $c_1 + c_2 > 1 \cap |c_1 - c_2| < 1$. The advantage of this equality is that, while the integrand on the left-hand side is wildly oscillating (see Fig. A.3), the integrand in the right-hand side is exponentially suppressed in the definition region such that a numerical evaluation is expected to be quickly convergent. This complete the picture in that it allows us to compute the weights $\mathcal{L}_k(c_1, c_2)$ in Eq. (A.26) for any positive value of c_1 and c_2, that is:

$$\mathcal{L}_k(c_1, c_2) = \begin{cases} \pi J_0(c_1\xi_k)J_0(c_2\xi_k)Y_0(\xi_k)\,, & c_1 + c_2 < 1\,, \\[2mm] 0\,, & |c_1 - c_2| > 1\,, \\[2mm] \frac{\pi}{2}[J_0(c_1\xi_k)J_0(c_2\xi_k) + Y_0(c_1\xi_k)Y_0(c_2\xi_k)]Y_0(\xi_k) & \\[2mm] + \frac{4}{\pi^2} \int_0^\infty \frac{dz\, z[K_0(c_1 z)K_0(c_2 z)I_0(z) + K_0(z)K_0(c_1 z)I_0(c_2) + K_0(c_2 z)K_0(z)I_0(c_1 z)]}{z^2 + \xi_k^2}\,, & \text{otherwise.} \end{cases}$$

(A.47)

A graphical representation of this weight as a function of c_1 and c_2 is shown in Fig. A.6 for $k = 1$.

We can now plug Eq. (A.47) into Eq. (A.25). Accounting for the rescaling factor h and defining for conve-
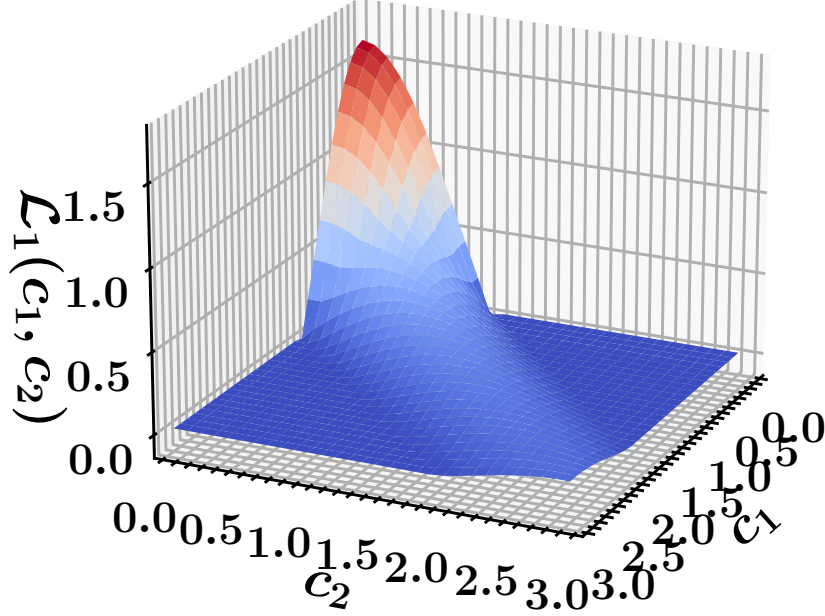
Fig. A.6: Graphical representation of Eq. (A.47) with $k = 1$.

nience $a_0 = 1$, after some manipulation it reads:

$$
\begin{aligned}
\int_{-\infty}^{\infty} dx\, |x| f(x) &= h \sum_{\substack{k=-\infty \\ k \neq 0}}^{\infty} |h\xi_k/a_0| f(h\xi_k/a_0) \frac{\theta(a_0 - |a_1 - a_2|)\mathcal{L}_k(a_1/a_0, a_2/a_0)}{a_0 J_1(a_0\xi_k/a_0) J_0(a_1\xi_k/a_0) J_0(a_2\xi_k/a_0)} \\[2mm]
&+ h \sum_{\substack{k=-\infty \\ k \neq 0}}^{\infty} |h\xi_k/a_1| f(h\xi_k/a_1) \frac{\theta(a_1 - |a_2 - a_0|)\mathcal{L}_k(a_2/a_1, a_0/a_1)}{a_1 J_1(a_1\xi_k/a_1) J_0(a_2\xi_k/a_1) J_0(a_0\xi_k/a_1)} \\[2mm]
&+ h \sum_{\substack{k=-\infty \\ k \neq 0}}^{\infty} |h\xi_k/a_2| f(h\xi_k/a_2) \frac{\theta(a_2 - |a_0 - a_1|)\mathcal{L}_k(a_0/a_2, a_1/a_2)}{a_2 J_1(a_2\xi_k/a_2) J_0(a_0\xi_k/a_2) J_0(a_1\xi_k/a_2)} .
\end{aligned}
\tag{A.48}
$$

We have also included θ-functions to limit the weights to the region where they are different from zero. Now we define the following list of pairs:

$$
\left\{ \left(\overline{\xi}_i = \frac{\xi_{k(i)}}{a_{n(i)}}, n(i), k(i) \right) \right\}, \quad i = -\infty, \ldots, \infty, \quad i \neq 0
\tag{A.49}
$$

in ascending order of $\overline{\xi}_i$, where $k(i)$ is the index of the zero of J_0 and $n(i) \in \{0, 1, 2\}$. With this definition at hand, Eq. (A.48) can be written in the following compact form:

$$
\int_{-\infty}^{\infty} dx\, |x| f(x) = h \sum_{\substack{i=-\infty \\ i \neq 0}}^{\infty} w_i |h\overline{\xi}_i| f(h\overline{\xi}_i),
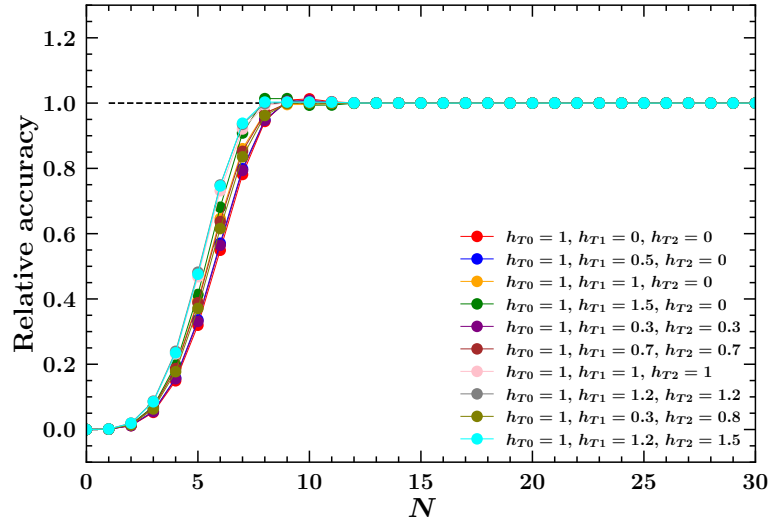\tag{A.50}
$$

Fig. A.7: Relative accuracy of the integral in Eq. (A.53) computed by means of Eq. (A.52) truncated to the N-th term.

where we have defined:

$$w_i = \frac{\theta(a_{n(i)} - |a_{n(i)+1} - a_{n(i)+2}|)\mathcal{L}_{k(i)}(a_{n(i)+1}/a_{n(i)}, a_{n(i)+2}/a_{n(i)})}{a_{n(i)}J_1(a_{n(i)}\overline{\xi}_i)J_0(a_{n(i)+1}\overline{\xi}_i)J_0(a_{n(i)+2}\overline{\xi}_i)} , \tag{A.51}$$

where $n(i) + 1$ and $n(i) + 2$ have to be interpreted as modulus 3, *i.e.* $1 + 2 \to 0$, $2 + 1 \to 0$, and $2 + 2 \to 1$.

The results above have been obtained assuming $a_1, a_2, a_1/a_2 \neq 1$. We now relax these assumptions in order to include all possible cases. In fact, one can show that this is easily accommodated by computing the weights w_i by setting $a_1 = 0$ if $a_1 = 1$, and $a_2 = 0$ if $a_2 = 1$ or if $a_2 = a_1$.[8]

We can now compute the integral in Eq. (A.20). As above, we make the change of variable in Eq. (A.16) so that:

$$\begin{aligned}
\mathcal{K}_0(h_{T0}, h_{T1}, h_{T2}) &= \frac{1}{h_{T0}}\frac{1}{h}\int_0^\infty dt\, \psi'\left(\frac{t}{\pi}\right) J_0\left(\frac{\pi}{h}\psi\left(\frac{t}{\pi}\right)\right) J_0\left(a_1\frac{\pi}{h}\psi\left(\frac{t}{\pi}\right)\right) J_0\left(a_2\frac{\pi}{h}\psi\left(\frac{t}{\pi}\right)\right) f\left(\frac{1}{h_{T0}}\frac{\pi}{h}\psi\left(\frac{t}{\pi}\right)\right) \\
&= \frac{1}{h_{T0}}\sum_{i=1}^\infty w_i \psi'\left(\frac{h\overline{\xi}_i}{\pi}\right) J_0\left(\frac{\pi}{h}\psi\left(\frac{h\overline{\xi}_i}{\pi}\right)\right) J_0\left(a_1\frac{\pi}{h}\psi\left(\frac{h\overline{\xi}_i}{\pi}\right)\right) J_0\left(a_2\frac{\pi}{h}\psi\left(\frac{h\overline{\xi}_i}{\pi}\right)\right) f\left(\frac{1}{h_{T0}}\frac{\pi}{h}\psi\left(\frac{h\overline{\xi}_i}{\pi}\right)\right)
\end{aligned}$$
$$\tag{A.52}$$

The sum in the second line is expected to converge fast to the true value of the integral as i increases. Therefore, truncating the series at a relative small value of i should provide a good approximation of the integral. Given the symmetry of $\mathcal{K}_0$ upon reshuffling h_{T0}, h_{T1}, and h_{T2}, without loss of generality one can always denote with h_{T0} the largest of all such that $a_1 = h_{T1}/h_{T0}$ and $a_2 = h_{T2}/h_{T0}$ are always such that $0 \leq a_i \leq 1$. This helps the convergence of the series.

To test this formula, we consider the integral:

$$\int_0^\infty db\, b J_0(h_{T0}b)J_0(h_{T1}b)J_0(h_{T2}b)e^{-\frac{b^2}{2}} . \tag{A.53}$$

Since we do not know how to solve it exactly, in Fig. A.7 we compare the convergence rate of this integral as a function of the truncation order N for different values of h_{T0}, h_{T1} and h_{T2} computed by means of Eq. (A.52) with $h = 10^{-2} \times \max[h_{T0}, h_{T1}, h_{T2}]$ to a brute-force numerical integration with high enough accuracy. Also in this case, the integral converges quickly to the true value within a few terms.

---

[8] In practice, in order to avoid divisions by zero, setting $a_1 = 0$ and/or $a_2 = 0$ really means setting these parameters to a small positive number.

B Cuts on the final-state leptons

In this section we derive explicitly the phase-space reduction factor $\mathcal{P}$ introduced in Sect. 2.1.1. This factor is defined as:

$$\mathcal{P}(Q, y, q_T) = \mathcal{P}(q) = \frac{\int_{\text{fid. reg.}} d^4p_1 d^4p_2 \, \delta(p_1^2)\delta(p_2^2)\theta(p_{1,0})\theta(p_{2,0})\delta^{(4)}(p_1 + p_2 - q)g_{\mu\nu}L^{\mu\nu}(p_1, p_2)}{\int d^4p_1 d^4p_2 \, \delta(p_1^2)\delta(p_2^2)\theta(p_{1,0})\theta(p_{2,0})\delta^{(4)}(p_1 + p_2 - q)g_{\mu\nu}L^{\mu\nu}(p_1, p_2)} \,, \tag{B.1}$$

where p_1 and p_2 are the four-momenta of the outgoing leptons and $L^{\mu\nu}$ is the leptonic tensor that, assuming massless leptons, reads:

$$L^{\mu\nu}(p_1, p_2) = 4(p_1^\mu p_2^\nu + p_2^\mu p_1^\nu - g^{\mu\nu}p_1 p_2) \,, \tag{B.2}$$

so that:

$$g_{\mu\nu}L^{\mu\nu}(p_1, p_2) = -8(p_1 p_2) = -4(p_1 + p_2)^2 \,. \tag{B.3}$$

In the last step we have used the on-shell-ness of the leptons ($p_1^2 = p_2^2 = 0$). The integral in the denominator of Eq. (B.1) is restricted to some *fiducial region*. Finally, we find:

$$\mathcal{P}(q) = \frac{\int_{\text{fid. reg.}} d^4p_1 d^4p_2 \, \delta(p_1^2)\delta(p_2^2)\theta(p_{1,0})\theta(p_{2,0})\delta^{(4)}(p_1 + p_2 - q)(p_1 + p_2)^2}{\int d^4p_1 d^4p_2 \, \delta(p_1^2)\delta(p_2^2)\theta(p_{1,0})\theta(p_{2,0})\delta^{(4)}(p_1 + p_2 - q)(p_1 + p_2)^2} \,. \tag{B.4}$$

The effect of integrating over the fiducial region can be implemented by defining a generalised θ-function, $\Phi(p_1, p_2)$, that is equal to one inside the fiducial region and zero outside. This allows one to integrate also the numerator of Eq. (B.4) over the full phase-space of the two outgoing leptons:

$$\mathcal{P}(q) = \frac{\int d^4p_1 d^4p_2 \, \delta(p_1^2)\delta(p_2^2)\theta(p_{1,0})\theta(p_{2,0})\delta^{(4)}(p_1 + p_2 - q)\Phi(p_1, p_2)(p_1 + p_2)^2}{\int d^4p_1 d^4p_2 \, \delta(p_1^2)\delta(p_2^2)\theta(p_{1,0})\theta(p_{2,0})\delta^{(4)}(p_1 + p_2 - q)(p_1 + p_2)^2} \,. \tag{B.5}$$

Now we can integrate over one of the outgoing momenta, say p_2, exploiting the momentum-conservation δ-function both in the numerator and in the denominator. Specifically, the numerator of Eq. (B.5) gives:

$$\int d^4p_1 d^4p_2 \, \delta(p_1^2)\delta(p_2^2)\theta(p_{1,0})\theta(p_{2,0})\delta^{(4)}(p_1 + p_2 - q)\Phi(p_1, p_2)(p_1 + p_2)^2 =$$

$$Q^2 \int d^4p_1 \delta(p_1^2)\delta((q - p_1)^2)\theta(p_{1,0})\theta(q_0 - p_{1,0})\Phi(p_1, q - p_1) \,, \tag{B.6}$$

and likewise in the denominator setting $\Phi(p_1, p_2) = 1$. Finally, renaming $p_1 = p$, the phase-space reduction factor reads:

$$\mathcal{P}(q) = \frac{\int d^4p \delta(p^2)\delta((q - p)^2)\theta(p_0)\theta(q_0 - p_0)\Phi(p, q - p)}{\int d^4p \delta(p^2)\delta((q - p)^2)\theta(p_0)\theta(q_0 - p_0)} \,. \tag{B.7}$$

The δ-functions can now be used to constrain two of the four components of the momentum p. The first, $\delta(p_2^2)$, is usually used to set the first component of p, the energy, to the on-shell value. Since the leptons are assumed to be massless, this produces:

$$\int d^4p \delta(p^2)\theta(p_0) = \int d^4p \delta(E^2 - |\mathbf{p}|^2)\theta(E) = \int \frac{dE d^3\mathbf{p}}{2|\mathbf{p}|}\delta(E - |\mathbf{p}|) = \int \frac{d^3\mathbf{p}}{2|\mathbf{p}|} \,. \tag{B.8}$$

Of course, the four-momentum p appearing in the rest of the integrand has to be set on shell ($E = |\mathbf{p}|$). Now we express the three-dimensional measure $d^3\mathbf{p}$ in spherical coordinates as:

$$d^3\mathbf{p} = |\mathbf{p}|^2 d|\mathbf{p}|d(\cos\theta)d\phi \,. \tag{B.9}$$

Then we make a change of variable from $(|\mathbf{p}|, \cos\theta)$ to $(|\mathbf{p}_T|, \eta)$: the second set of variables are exactly those on which kinematic cuts are imposed. We do so by knowing that:

$$
\begin{cases} |\mathbf{p}| = |\mathbf{p}_T| \cosh\eta \,, \\ \cos\theta = \tanh\eta \,. \end{cases}
\tag{B.10}
$$

This leads to:

$$
\int \frac{d^3\mathbf{p}}{2|\mathbf{p}|} = \frac{1}{2} \int |\mathbf{p}| d|\mathbf{p}| d(\cos\theta) d\phi = \frac{1}{2} \int |\mathbf{p}_T| d|\mathbf{p}_T| d\eta d\phi = \frac{1}{2} \int d^2\mathbf{p}_T d\eta \,.
\tag{B.11}
$$

Now we consider the second δ-function:

$$
\frac{1}{2} \int d^2\mathbf{p}_T d\eta \, \delta((q-p)^2)\theta(q_0 - p_0) = \frac{1}{2} \int_{-\infty}^{\infty} d\eta \int_0^{2\pi} d\phi \int_0^{\infty} |\mathbf{p}_T| d|\mathbf{p}_T| \, \delta(Q^2 - 2p\cdot q)\theta(q_0 - p_0) \,,
\tag{B.12}
$$

being $q^2 = Q^2$ and $p^2 = 0$. It is convenient to express the four-vector q in terms of Q, y, and $\mathbf{q}_T$:

$$
q = (M\cosh y, \mathbf{q}_T, M\sinh y) \,.
\tag{B.13}
$$

with $M = \sqrt{Q^2 + |\mathbf{q}_T|^2}$. While:

$$
p = (|\mathbf{p}_T|\cosh\eta, \mathbf{p}_T, |\mathbf{p}_T|\sinh\eta) \,,
\tag{B.14}
$$

so that:

$$
p\cdot q = |\mathbf{p}_T|M(\cosh\eta\cosh y - \sinh\eta\sinh y) - \mathbf{p}_T\cdot\mathbf{q}_T = |\mathbf{p}_T|M\cosh(\eta - y) - \mathbf{p}_T\cdot\mathbf{q}_T \,.
\tag{B.15}
$$

We can now assume that the two-dimensional vector $\mathbf{q}_T$ is aligned with the x axis so that $\mathbf{p}_T\cdot\mathbf{q}_T = |\mathbf{p}_T||\mathbf{q}_T|\cos\phi$[9]. Therefore, the argument of the δ-function in Eq. (B.12) becomes:

$$
f(|\mathbf{p}_T|, \eta, \phi) = Q^2 - 2|\mathbf{p}_T|\left[M\cosh(\eta - y) - |\mathbf{q}_T|\cos\phi\right] \,.
\tag{B.16}
$$

and that of the ϑ-function $M\cosh y - |\mathbf{p}_T|\cosh\eta$. It thus appears convenient to integrate Eq. (B.12) over $|\mathbf{p}_T|$ first:

$$
\frac{1}{2} \int_0^{\infty} |\mathbf{p}_T| d|\mathbf{p}_T| \, \delta(Q^2 - 2p\cdot q)\theta(q_0 - p_0) = \frac{\bar{p}_T^2}{2Q^2}\vartheta(M\cosh y - \bar{p}_T\cosh\eta) = \frac{\bar{p}_T^2}{2Q^2} \,,
\tag{B.17}
$$

with[10]:

$$
\bar{p}_T(\cos\phi) = \frac{Q^2}{2\left[M\cosh(\eta - y) - |\mathbf{q}_T|\cos\phi\right]} = \frac{Q^2}{2|\mathbf{q}_T|}\frac{1}{\left[\frac{M\cosh(\eta - y)}{|\mathbf{q}_T|} - \cos\phi\right]} \,.
\tag{B.18}
$$

Now we turn to consider the integral in $d\phi$. To this end, the following relations are useful:

$$
\int_0^{2\pi} d\phi \, f(\cos\phi) = \int_{-1}^1 \frac{dx}{\sqrt{1 - x^2}}\left[f(x) + f(-x)\right] \,.
\tag{B.19}
$$

and:

$$
\int \frac{dx}{(a \pm x)^2\sqrt{1 - x^2}} = \frac{\sqrt{1 - x^2}}{(a^2 - 1)(x \pm a)} \pm \frac{2a}{(a^2 - 1)^{3/2}}\tan^{-1}\left(\frac{x \pm a(1 - \sqrt{1 - x^2})}{\sqrt{a^2 - 1}x}\right) \,.
\tag{B.20}
$$

The last integral is such that:

$$
\int_{-1}^1 \frac{dx}{(a \pm x)^2\sqrt{1 - x^2}} = \frac{\pi a}{(a^2 - 1)^{3/2}} \,.
\tag{B.21}
$$

---

[9] In the general case in which $\mathbf{q}_T$ forms an angle β with the x axis, the scalar product would result in $|\mathbf{p}_T||\mathbf{q}_T|\cos(\phi - \beta)$. However, the angle β could always be reabsorbed in a redefinition of the integration angle ϕ in Eq. (B.12).

[10] Notice that the ϑ-function has no effect. I have verified it numerically but I cannot see it analytically.

We now use Eqs. (B.19)-(B.21) to compute:

$$
\frac{1}{2Q^2} \int_0^{2\pi} d\phi \, [\overline{p}_T(\cos\phi)]^2 = \frac{Q^2}{8|\mathbf{q}_T|^2} \int_0^{2\pi} \frac{d\phi}{\left[\frac{M\cosh(\eta-y)}{|\mathbf{q}_T|} - \cos\phi \right]^2}
$$

$$
= \frac{Q^2}{8|\mathbf{q}_T|^2} \int_{-1}^{1} \frac{dx}{\sqrt{1-x^2}} \left[\frac{1}{\left(\frac{M\cosh(\eta-y)}{|\mathbf{q}_T|} - x \right)^2} + \frac{1}{\left(\frac{M\cosh(\eta-y)}{|\mathbf{q}_T|} + x \right)^2} \right]
$$

$$
= \frac{Q^2}{8} \left\{ \frac{2|\mathbf{q}_T|^2 x \sqrt{1-x^2}}{(M^2\cosh^2(\eta-y) - |\mathbf{q}_T|^2)(x^2|\mathbf{q}_T|^2 - M^2\cosh^2(\eta-y))} \right. \tag{B.22}
$$

$$
+ \left. \frac{2M\cosh(\eta-y)}{(M^2\cosh^2(\eta-y) - |\mathbf{q}_T|^2)^{3/2}} \left[\tan^{-1}\left(\frac{x\sqrt{(M^2\cosh^2(\eta-y) - |\mathbf{q}_T|^2)}}{M\cosh(\eta-y)\sqrt{1-x^2}} \right) \right] \right\}_{-1}^{1}
$$

$$
= \frac{\pi Q^2 M \cosh(\eta-y)}{4(M^2\cosh^2(\eta-y) - |\mathbf{q}_T|^2)^{3/2}}
$$

We can go further and solve also the integral in η:

$$
\int d^4 p \, \delta(p^2) \delta((q-p)^2) \theta(p_0) \theta(q_0 - p_0) = \int_{-\infty}^{\infty} d\eta \frac{\pi Q^2 M \cosh(\eta-y)}{4(M^2\cosh^2(\eta-y) - |\mathbf{q}_T|^2)^{3/2}} =
$$

$$
\frac{\pi}{4} \frac{Q^2}{M^2} \int_{-\infty}^{\infty} \frac{d(\sinh\eta)}{\left(\sinh^2(\eta-y) + \frac{Q^2}{M^2} \right)^{3/2}} = \frac{\pi}{4} \frac{Q^2}{M^2} \left[\frac{M^2}{Q^2} \frac{\sinh\eta}{\sqrt{\sinh^2\eta + \frac{Q^2}{M^2}}} \right]_{-\infty}^{\infty} = \frac{\pi}{2} . \tag{B.23}
$$

Remarkably, this result gives us the denominator of Eq. (B.7). We now need to compute the numerator by inserting the appropriate function Φ. In our case, the kinematic cuts are identical for the outgoing leptons and read:

$$
\eta_{\min} < \eta_{1(2)} < \eta_{\max} \quad \text{and} \quad |\mathbf{p}_{T,1(2)}| > p_{T,\min} . \tag{B.24}
$$

Therefore, the function Φ factorises into two identical functions as:

$$
\Phi(p_1, p_2) = \Theta(p_1)\Theta(p_2) , \tag{B.25}
$$

with:

$$
\Theta(p) = \vartheta(\eta - \eta_{\min})\vartheta(\eta_{\max} - \eta)\vartheta(|\mathbf{p}_T| - p_{T,\min}) . \tag{B.26}
$$

Referring to Eq. (B.7) and considering that:

$$
q - p = (M\cosh y - |\mathbf{p}_T|\cosh\eta, \, \mathbf{q}_T - \mathbf{p}_T, \, M\sinh y - |\mathbf{p}_T|\sinh\eta) . \tag{B.27}
$$

we thus have:

$$\Phi(p, q - p) = \Theta(p)\Theta(q - p) =$$

$$\vartheta(\eta - \eta_{\min})\vartheta(\eta_{\max} - \eta) \times$$

$$\vartheta(|\mathbf{p}_T| - p_{T,\min}) \times$$

$$\vartheta\left(\frac{1}{2}\ln\left(\frac{M\cosh y - |\mathbf{p}_T|\cosh\eta + M\sinh y - |\mathbf{p}_T|\sinh\eta}{M\cosh y - |\mathbf{p}_T|\cosh\eta - M\sinh y + |\mathbf{p}_T|\sinh\eta}\right) - \eta_{\min}\right) \times$$

$$\vartheta\left(\eta_{\max} - \frac{1}{2}\ln\left(\frac{M\cosh y - |\mathbf{p}_T|\cosh\eta + M\sinh y - |\mathbf{p}_T|\sinh\eta}{M\cosh y - |\mathbf{p}_T|\cosh\eta - M\sinh y + |\mathbf{p}_T|\sinh\eta}\right)\right) \times$$

$$\vartheta(|\mathbf{q}_T - \mathbf{p}_T| - p_{T,\min}) = \tag{B.28}$$

$$1): \quad \vartheta(\eta - \eta_{\min}) \times \vartheta(\eta_{\max} - \eta) \times$$

$$2): \quad \vartheta(\overline{p}_T - p_{T,\min}) \times$$

$$3): \quad \vartheta\left(\frac{1}{2}\ln\left(\frac{Me^y - \overline{p}_T e^\eta}{Me^{-y} - \overline{p}_T e^{-\eta}}\right) - \eta_{\min}\right) \times \vartheta\left(\eta_{\max} - \frac{1}{2}\ln\left(\frac{Me^y - \overline{p}_T e^\eta}{Me^{-y} - \overline{p}_T e^{-\eta}}\right)\right) \times$$

$$4): \quad \vartheta(\sqrt{|\mathbf{q}_T|^2 + \overline{p}_T^2 - 2|\mathbf{q}_T|\overline{p}_T\cos\phi} - p_{T,\min}),$$

where in the last step we have replaced $|\mathbf{p}_T|$ with $\overline{p}_T$ defined Eq. (B.18). Now the question is identifying the integration domain defined by $\Phi(p, q - p)$ on the $(\eta, \cos\phi)$-plane. Since the θ-functions in Eq. (B.7) will be used inside a double nested integral over $x = \cos\phi$ first and η second, it is convenient to rewrite the function $\Phi(p, q - p)$ in Eq. (B.28) as follows:

$$\begin{aligned}
\Phi(p, q - p) &= \vartheta(\eta - \eta_{\min}) \times \vartheta(\eta_{\max} - \eta) \\
&\times \vartheta(x - f^{(2)}(\eta, p_{T,\min})) \\
&\times \vartheta(f^{(3)}(\eta, \eta_{\min}) - x) \times \vartheta(f^{(3)}(\eta, \eta_{\max}) - x) \\
&\times \vartheta(f^{(4)}(\eta, p_{T,\min}) - x),
\end{aligned} \tag{B.29}$$

with:

$$\begin{aligned}
f^{(2)}(\eta, p_{T,\text{cut}}) &= \frac{2Mp_{T,\text{cut}}\cosh(\eta - y) - Q^2}{2p_{T,\text{cut}}|\mathbf{q}_T|}, \\
f^{(3)}(\eta, \eta_{\text{cut}}) &= \frac{M\cosh(\eta - y)}{|\mathbf{q}_T|} - \frac{Q^2\left(\sinh(\eta - y)\coth(y - \eta_{\text{cut}}) + \cosh(\eta - y)\right)}{2|\mathbf{q}_T|M}, \\
f^{(4)}(\eta, p_{T,\text{cut}}) &= \frac{M\cosh(\eta - y)(Q^2 - 2p_{T,\text{cut}}^2 + 2|\mathbf{q}_T|^2) - Q^2\sqrt{M^2\sinh^2(\eta - y) + p_{T,\text{cut}}^2}}{2|\mathbf{q}_T|\left(M^2 - p_{T,\text{cut}}^2\right)}.
\end{aligned} \tag{B.30}$$

Considering that $-1 \leq \cos\phi \leq 1$, the integration domain is limited to this region. Therefore, Eq. (B.29) can be written in an even more convenient way as:

$$\begin{aligned}
\Phi(p, q - p) &= \vartheta(\eta - \eta_{\min})\vartheta(\eta_{\max} - \eta) \\
&\times \vartheta(x - \max[f^{(2)}(\eta, p_{T,\min}), -1]) \\
&\times \vartheta(\min[f^{(3)}(\eta, \eta_{\min}), f^{(3)}(\eta, \eta_{\max}), f^{(4)}(\eta, p_{T,\min}), 1] - x)
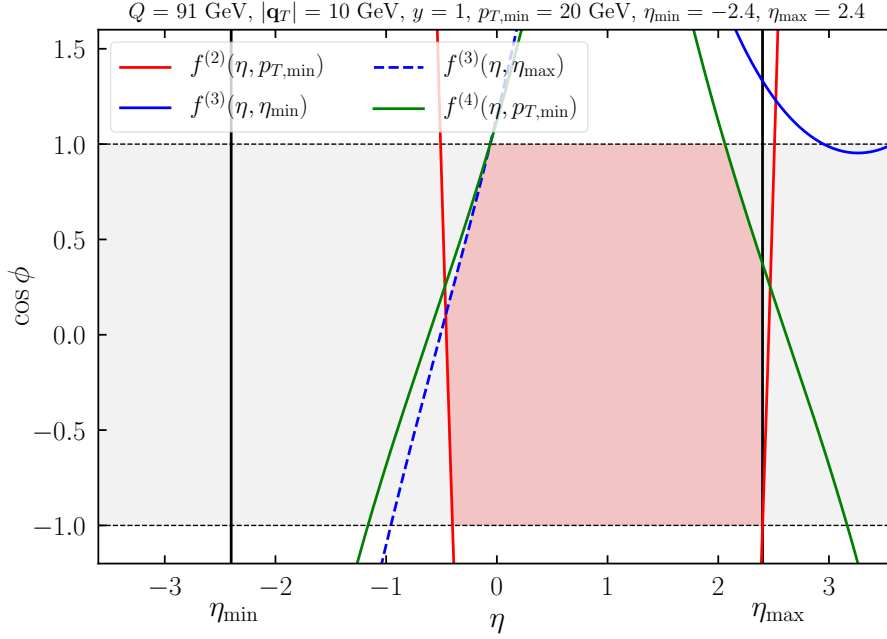\end{aligned} \tag{B.31}$$

Fig. B.1: The red area indicates the integration domain of the numerator in of the phase-space reduction factor Eq. (B.7) for $p_{T,\mathrm{min}} = 20$ GeV and $-\eta_{\mathrm{min}} = \eta_{\mathrm{max}} = 2.4$ at $Q = 91$ GeV, $|\mathbf{q}_T| = 10$ GeV and $y = 1$.

such that a double integral over η and x would read:

$$\int_{-\infty}^{\infty} d\eta \int_{-1}^{1} dx\, \Phi(p, q-p) \cdots = \int_{\eta_{\mathrm{min}}}^{\eta_{\mathrm{max}}} d\eta\, \vartheta(x_2(\eta) - x_1(\eta)) \int_{x_1(\eta)}^{x_2(\eta)} dx \ldots \,. \tag{B.32}$$

with:

$$x_1(\eta) = \max[f^{(2)}(\eta, p_{T,\mathrm{min}}), -1] \tag{B.33}$$

and:

$$x_2(\eta) = \min[f^{(3)}(\eta, \eta_{\mathrm{min}}), f^{(3)}(\eta, \eta_{\mathrm{max}}), f^{(4)}(\eta, p_{T,\mathrm{min}}), 1]\,. \tag{B.34}$$

As an example, Fig. B.1 shows the integration domain of the numerator in of the phase-space reduction factor Eq. (B.7) for $p_{T,\mathrm{min}} = 20$ GeV and $-\eta_{\mathrm{min}} = \eta_{\mathrm{max}} = 2.4$ at $Q = 91$ GeV, $|\mathbf{q}_T| = 10$ GeV and $y = 1$. The gray band corresponds to the region $1 \leq \cos\phi \leq 1$. The θ-function 1) in Eq. (B.28) limits the region to the vertical stip defined by $\eta_{\mathrm{min}} < \eta < \eta_{\mathrm{max}}$ (black vertical lines), the θ-function 2) gives the red lines, the θ-functions 3) the blue lines , and the θ-function 4) the green lines.

Gathering all pieces, the final expression for the phase-space reduction factor reads:

$$\mathcal{P}(Q, y, q_T) = \int_{\eta_{\mathrm{min}}}^{\eta_{\mathrm{max}}} d\eta\, \vartheta(x_2(\eta) - x_1(\eta)) \left[F(x_2(\eta), \eta) - F(x_1(\eta), \eta) \right] \tag{B.35}$$

with:

$$F(x, \eta) = \frac{1}{4\pi} \frac{Q^2}{E_q^2 - q_T^2} \left\{ \frac{2q_T^2 x\sqrt{1 - x^2}}{x^2 q_T^2 - E_q^2} + \frac{2E_q}{\sqrt{E_q^2 - q_T^2}} \left[\tan^{-1}\left(\frac{x\sqrt{E_q^2 - q_T^2}}{\sqrt{1 - x^2}\, E_q} \right) \right] \right\} \tag{B.36}$$

where we have defined $E_q = M\cosh(\eta - y)$ and $q_T = |\mathbf{q}_T|$.

Let us consider the case $y = q_T = 0$. For simplicity, we also take $\eta_{\mathrm{min}} = -\eta_{\mathrm{max}}$. In these conditions, Eq. (B.36) reduces to:

$$F(x, \eta) = \frac{1}{2\pi} \frac{1}{\cosh^2(\eta)} \left[\tan^{-1}\left(\frac{x}{\sqrt{1 - x^2}} \right) \right]\,. \tag{B.37}$$

As evident from Eq. (B.30), for $q_T = 0$ all functions $f^{(2)}$, $f^{(3)}$, and $f^{(4)}$ diverge. The relevant question, though, is whether they go to plus or minus infinity depending on the value of Q. Of course, q_T will tend to zero positively so we find:

$$f^{(2)}(\eta, p_{T,\mathrm{min}}) \to \infty \times \mathrm{sign}\left[2p_{T,\mathrm{min}}\cosh(\eta) - Q\right],$$

$$f^{(3)}(\eta, \eta_{\mathrm{min}} = -\eta_{\mathrm{max}}) \to +\infty$$

$$f^{(3)}(\eta, \eta_{\mathrm{max}}) \to -\infty,\tag{B.38}$$

$$f^{(4)}(\eta, p_{T,\mathrm{min}}) \to \infty \times \mathrm{sign}\left[\frac{\cosh(\eta)(Q^2 - 2p_{T,\mathrm{min}}^2) - Q\sqrt{Q^2\sinh^2(\eta) + p_{T,\mathrm{min}}^2}}{Q^2 - p_{T,\mathrm{min}}^2}\right],$$

Therefore, $f^{(3)}$ never actually contributes. In addition, for the θ-function in Eq. (B.35) to be different from zero, we need $f^{(2)}(\eta) \to -\infty$ and $f^{(3)}(\eta) \to \infty$. These both translate into $Q \geq 2p_{T,\mathrm{min}}\cosh(\eta)$. This inequality is satisfied only if $Q \geq 2p_{T,\mathrm{min}}$ for:

$$-\overline{\eta} \leq \eta \leq \overline{\eta} \quad \text{with} \quad \overline{\eta} = \cosh^{-1}\left(\frac{Q}{2p_{T,\mathrm{min}}}\right).\tag{B.39}$$

Therefore, the phase-space reduction factor eventually becomes:

$$\begin{aligned}
\mathcal{P}(Q,0,0) &= \frac{1}{2}\vartheta(Q - 2p_{T,\mathrm{min}})\int_{-\eta_{\mathrm{max}}}^{\eta_{\mathrm{max}}}\frac{d\eta}{\cosh^2\eta}\,\vartheta(\eta + \overline{\eta})\vartheta(\overline{\eta} - \eta) \\
&= \vartheta(Q - 2p_{T,\mathrm{min}})\tanh(\max[\eta_{\mathrm{max}},\overline{\eta}]).
\end{aligned}\tag{B.40}$$

This result can be written more explicitly as:

$$\mathcal{P}(Q,0,0) = \begin{cases} 0 & Q < 2p_{T,\mathrm{min}}, \\ \tanh(\overline{\eta}) = \left(1 + \dfrac{2p_{T,\mathrm{min}}}{Q}\right)\sqrt{1 - \dfrac{4p_{T,\mathrm{min}}}{Q + 2p_{T,\mathrm{min}}}} & 2p_{T,\mathrm{min}} \leq Q < 2p_{T,\mathrm{min}}\cosh\eta_{\mathrm{max}}, \\ \tanh(\eta_{\mathrm{max}}) & Q \geq 2p_{T,\mathrm{min}}\cosh\eta_{\mathrm{max}}. \end{cases}\tag{B.41}$$

This differs from Eq. (24) of Ref. [1]. Despite the three different regions coincide, the behavior of the phase-space reduction factor for all regions but for $Q < 2p_{T,\mathrm{min}}$ is different. In favour of our result there is the fact that $\mathcal{P}(Q,0,0)$ in Eq. (B.41) is continuous at $Q = 2p_{T,\mathrm{min}}\cosh\eta_{\mathrm{max}}$ while that of Ref. [1] is not. In addition, when setting $p_{T,\mathrm{min}} = 0$ and $\eta_{\mathrm{max}} = \infty$, i.e. no cuts, our result tends to $\mathcal{P}(Q,0,0) = \tanh(\infty) = 1$, as it should. While the result in Eq. (24) of Ref. [1] actually diverges in this limit.

The integrand of Eq. (B.35), due to the behaviour of x_1 and x_2 as functions of η, a piecewise function. Therefore, its numerical integration is problematic in that quadrature algorithms assume the integrand be continuos over the integration range. The solution is to identify the discontinuity points and integrate the function separately over the resulting ranges. However, the complexity of the integration region (e.g. see Fig. B.1) makes the analytical identification of the discontinuity points very hard to achieve.

B.1   Contracting the leptonic tensor with $g_\perp^{\mu\nu}$

The calculation done in the previous section holds when contracting the leptonic tensor $L_{\mu\nu}$ with the metric tensor $g^{\mu\nu}$ associated with the Lorentz structure of the hadronic tensor. However, at small values of $|\mathbf{q}_T|$, the leading-power Lorentz structure that one needs to multiply the leptonic tensor for is:

$$g_\perp^{\mu\nu} = g^{\mu\nu} + z^\mu z^\nu - t^\mu t^\nu\tag{B.42}$$

where the vectors z^μ and t^μ in the Collins-Soper (CS) frame are defined as:

$$z^\mu = (\sinh y, \mathbf{0}, \cosh y),$$

$$t^\mu = \frac{q^\mu}{Q},\tag{B.43}$$

and they are such that $z^2 = -1$, $t^2 = 1$ and $zq = 0$. If we use the on-shell-ness of p_1 and p_2 ($p_1^2 = p_2^2 = 0$) and the momentum conservation ($p \equiv p_1$, $p_2 = q - p$), we find that $t^\mu t^\nu L_{\mu\nu} = 0$ and the quantity above reduces to:

$$L_\perp = g_\perp^{\mu\nu} L_{\mu\nu} = 4 \left[\frac{1}{2} q^2 + 2(zp)^2 \right] = 2Q^2 \left[1 + 4 \sinh^2(y - \eta) \frac{|\mathbf{p}_T|^2}{Q^2} \right] . \tag{B.44}$$

Therefore, we need to introduce this factor in both the numerator and the denominator of Eq. (B.7). Following the same steps of the previous section, up to a factor $2Q^2$, this leads us to replace the integral in Eq. (B.17) with([11]):

$$\frac{1}{2} \int_0^\infty |\mathbf{p}_T| \left[1 + 4 \sinh^2(y - \eta) \frac{|\mathbf{p}_T|^2}{Q^2} \right] d|\mathbf{p}_T| \delta(Q^2 - 2p \cdot q) = \frac{\overline{p}_T^2}{2Q^2} + 2 \sinh^2(y - \eta) \frac{\overline{p}_T^4}{Q^4} . \tag{B.45}$$

We can still use Eq. (B.20) for the first term in the r.h.s. of the equation above. For the second, instead we need to use:

$$\int \frac{dx}{(a \pm x)^4 \sqrt{1 - x^2}} = \frac{\sqrt{1 - x^2} \left[(11a^2 + 4)x^2 \pm 3a(9a^2 + 1)x + (18a^4 - 5a^2 + 2) \right]}{6(a^2 - 1)^3(x \pm a)^3}$$
$$\pm \frac{a(2a^2 + 3)}{2(a^2 - 1)^{7/2}} \tan^{-1} \left(\frac{x \pm a(1 - \sqrt{1 - x^2})}{\sqrt{a^2 - 1}x} \right) , \tag{B.46}$$

that is such that:

$$\int_{-1}^1 \frac{dx}{(a \pm x)^4 \sqrt{1 - x^2}} = \frac{\pi a(2a^2 + 3)}{2(a^2 - 1)^{7/2}} . \tag{B.47}$$

In our particular case, the integrand we are considering is the second term in the r.h.s. term of Eq. (B.45):

$$\frac{2 \sinh^2(y - \eta)}{Q^4} \int_0^{2\pi} d(\phi) \overline{p}_T^4 (\cos \phi) =$$

$$\frac{Q^4}{8q_T^4} \sinh^2(y - \eta) \int_{-1}^1 \frac{dx}{\sqrt{1 - x^2}} \left[\frac{1}{(a + x)^4} + \frac{1}{(a - x)^4} \right] = \frac{\pi Q^4}{8q_T^4} \sinh^2(y - \eta) \frac{a(2a^2 + 3)}{(a^2 - 1)^{7/2}} . \tag{B.48}$$

with:

$$a = \frac{M}{q_T} \cosh(y - \eta) . \tag{B.49}$$

Now we need to integrate Eq. (B.48) over η:

$$\frac{\pi Q^4}{8q_T^4} \int_{-\infty}^\infty d\eta \sinh^2(y - \eta) \frac{a(2a^2 + 3)}{(a^2 - 1)^{7/2}} . \tag{B.50}$$

If we make the following change of variable in the integral above:

$$z = \frac{M}{q_T} \sinh(y - \eta) \tag{B.51}$$

such that:

$$a^2 = z^2 + \frac{M^2}{q_T^2} \quad \text{and} \quad dz = -a d\eta , \tag{B.52}$$

the integral above becomes:

$$\frac{\pi Q^4}{4M^2 q_T^2} \int_{-\infty}^\infty dz \frac{z^2 \left(z^2 + \frac{M^2}{q_T^2} + \frac{3}{2} \right)}{\left(z^2 + \frac{M^2}{q_T^2} - 1 \right)^{7/2}} = \frac{\pi}{6} . \tag{B.53}$$

Putting this result together with Eq. (B.23) and taking into account the factor $2Q^2$ in Eq. (B.44), we find that:

$$\int d^4 p \delta(p^2) \delta((q - p)^2) \theta(p_0) \theta(q_0 - p_0) L_\perp = \frac{4\pi}{3} Q^2 . \tag{B.54}$$

---

[11] We removed the θ-function as we know it does not have any effect.

This result agrees with Eq. (2.38) of Ref. [1], up to a factor four. This provides the denominator of the phase-space-reduction factor $\mathcal{P}$. The structure of $\mathcal{P}$ will be exactly like that in Eq. (B.35), the only thing we need to do is to identify the correct function $F(x, \eta)$. To this end, we need to make the following replacement for the function F given in Eq. (B.36) with:

$$F(x, \eta) \to \overline{F}(x, \eta) = \frac{3}{4} F(x, \eta) + \frac{1}{4} G(x, \eta) \,, \tag{B.55}$$

where:

$$
\begin{aligned}
G(x, \eta) &= \frac{1}{16\pi} \sinh^2(y - \eta) \frac{Q^4}{(E_q^2 - q_T^2)^3} \left\{ \frac{2x\sqrt{1 - x^2} q_T^2}{(x^2 q_T^2 - E_q^2)^3} \right. \\[2mm]
&\times \left[q_T^4 (11 E_q^2 q_T^2 + 4 q_T^4) x^4 - 2 q_T^2 (15 E_q^4 + E_q^2 q_T^2 - q_T^4) x^2 + 3 E_q^2 (9 E_q^4 - 6 E_q^2 q_T^2 + 2 q_T^4) \right] \\[2mm]
&+ \left. \frac{6 E_q (2 E_q^2 + 3 q_T^2)}{\sqrt{E_q^2 - q_T^2}} \left[\tan^{-1} \left(\frac{x\sqrt{E_q^2 - q_T^2}}{\sqrt{1 - x^2} E_q} \right) \right] \right\} \,.
\end{aligned}
\tag{B.56}
$$

Finally, combining the functions F and G given in Eqs. (B.36) and (B.56), respectively, according to Eq. (B.55) to obtain $\overline{F}$, and replacing F with $\overline{F}$ in Eq. (B.35) gives the phase-space-reduction factor $\mathcal{P}(Q, y, q_T)$ when the leptonic tensor $L_{\mu\nu}$ is contracted with the transverse metrics $g_\perp^{\mu\nu}$.

As a final check, it is interesting to compute $\mathcal{P}$ when $y = q_T = 0$, again assuming $\eta_{\min} = -\eta_{\max}$. In this limit F reduces to the expression in Eq. (B.37), while G becomes:

$$G(x, \eta) = \frac{3}{2\pi} \frac{\sinh^2(\eta)}{\cosh^4(\eta)} \left[\tan^{-1} \left(\frac{x}{\sqrt{1 - x^2}} \right) \right] \,, \tag{B.57}$$

such that:

$$
\begin{aligned}
\mathcal{P}(Q, 0, 0) &= \frac{3}{8} \vartheta(Q - 2 p_{T,\min}) \int_{-\eta_{\max}}^{\eta_{\max}} d\eta \left[\frac{\cosh^2(\eta) + \sinh^2(\eta)}{\cosh^4(\eta)} \right] \vartheta(\eta + \overline{\eta}) \vartheta(\overline{\eta} - \eta) \\[2mm]
&= \vartheta(Q - 2 p_{T,\min}) \tanh(\max[\eta_{\max}, \overline{\eta}]) \left[1 - \frac{1}{4 \cosh^2(\max[\eta_{\max}, \overline{\eta}])} \right] \,,
\end{aligned}
\tag{B.58}
$$

with $\overline{\eta}$ defined in Eq. (B.39). The relation above can be written more explicitly as:

$$
\mathcal{P}(Q, 0, 0) = \begin{cases} 0 & Q < 2 p_{T,\min} \,, \\ \tanh(\overline{\eta}) \left[1 - \frac{1}{4 \cosh^2(\overline{\eta})} \right] = \left(1 - \frac{p_{T,\min}^2}{Q^2} \right) \sqrt{1 - \frac{4 p_{T,\min}^2}{Q^2}} & 2 p_{T,\min} \leq Q < 2 p_{T,\min} \cosh \eta_{\max} \,, \\ \tanh(\eta_{\max}) \left[1 - \frac{1}{4 \cosh^2(\eta_{\max})} \right] & Q \geq 2 p_{T,\min} \cosh \eta_{\max} \,. \end{cases}
\tag{B.59}
$$

The reason why we kept $\eta_{\min} \neq -\eta_{\max}$ is that in some cases it may be required to implement an asymmetric cut, $\eta_{\min} < \eta < \eta_{\max}$. This is the case, for example, of the LHCb experiment that delivers data only in the forward region ($2 < \eta < 4.5$). As an example, Fig. B.2 shows the integration domain of the phase-space reduction factor Eq. (B.7) for $p_{T,\min} = 20$ GeV and $2 < \eta < 4.5$ at $Q = 91$ GeV, $|\mathbf{q}_T| = 10$ GeV and $y = 3$.

B.2 Parity-violating contribution

In the presence of cuts on the final-state leptons and for invariant masses around the Z mass, parity-violating effects arise. As we will show below, these effects integrate to zero when removing the leptonic cuts. This contribution stems from interference of the antisymmetric contributions to the lepton tensor, proportional to $p_1^\mu p_2^\nu \epsilon_{\mu\nu\rho\sigma}$, and the hadronic tensor, proportional to $\epsilon_\perp^{\mu\nu}$ defined as:

$$\epsilon_\perp^{\mu\nu} \equiv \epsilon^{\mu\nu\rho\sigma} t_\rho z_\sigma \,, \tag{B.60}$$

where t^μ and z^μ are given in Eq. (B.43). Therefore, the contribution we are after results from the contraction of the following Lorentz structures:

$$L_{\text{PV}} \equiv p_1^\mu p_2^\nu \epsilon_{\mu\nu\rho\sigma} \epsilon_\perp^{\rho\sigma} \,. \tag{B.61}$$
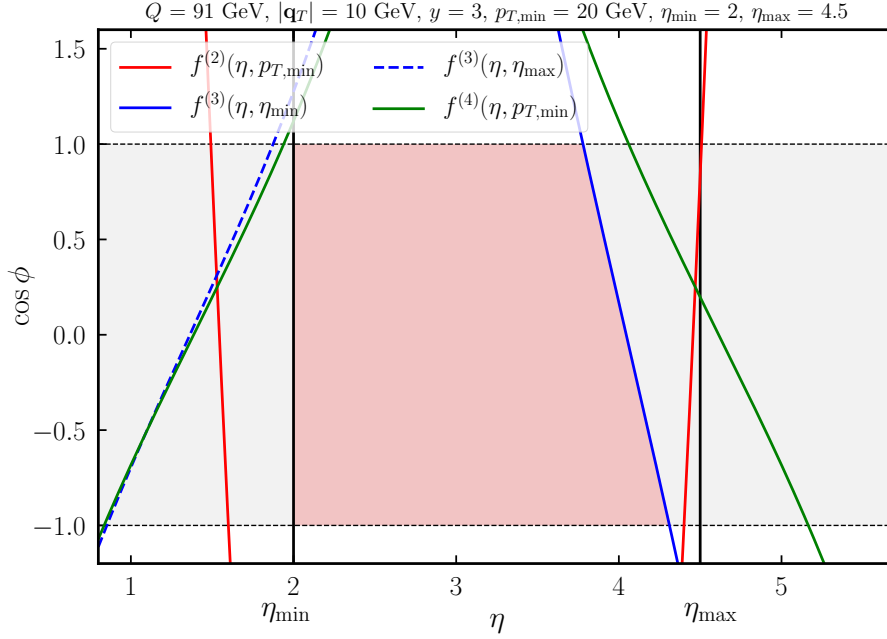
Fig. B.2: Same as Fig. B.1 for the asymmetric rapidity cut $2 < \eta < 4.5$ at $y = 3$.

After some manipulation, one finds:

$$
\begin{aligned}
L_{\text{PV}} &= p_1^\mu p_2^\nu \epsilon_{\mu\nu\rho\sigma} \epsilon^{\rho\sigma\alpha\beta} t_\alpha z_\beta = -2 p_1^\mu p_2^\nu \delta_\mu^\alpha \delta_\nu^\beta t_\alpha z_\beta \\[2mm]
&= -2(p_1 t)(p_2 z) = -2(pt)\left[(qz) - (pz)\right] = 2(pt)(pz) \\[2mm]
&= \frac{2|\mathbf{p}_T|^2}{Q} \sinh(y - \eta) \left[M \cosh(y - \eta) - |\mathbf{q}_T| \cos\phi \right] ,
\end{aligned}
\tag{B.62}
$$

where I have defined $p_1 \equiv p$ and used the equalities $p_2 = q - p$, and $zq = 0$. To compute the third line I have used the explicit parameterisation of q and p given in Eqs. (B.13) and (B.14), respectively. The presence of $\sinh(y - \eta)$ in Eq. (B.62) is such that integrating over the full range in the lepton rapidity η nullifies this contribution:

$$
\int_{-\infty}^{\infty} d\eta \, L_{\text{PV}} = 0 .
\tag{B.63}
$$

Therefore, it turns out that, for observables inclusive in the lepton phase space, the parity violating term does not give any contribution. Conversely, the presence of cuts on the final-state leptons may prevent Eq. (B.63) from being satisfied leaving a residual contribution. In order to quantify this effect, we take the same steps performed in the previous sections to integrate L_{PV} over the fiducial region. As above, we start integrating over the full range in $|\mathbf{p}_T|$ using the on-shell-ness δ-function:

$$
\begin{aligned}
\int_0^\infty d|\mathbf{p}_T| |\mathbf{p}_T| \, L_{\text{PV}} &= \frac{\sinh(y - \eta)}{Q} \left[M \cosh(y - \eta) - |\mathbf{q}_T| \cos\phi \right] \int_0^\infty d|\mathbf{p}_T| |\mathbf{p}_T|^3 \delta(Q^2 - 2pq) \\[2mm]
&= \frac{\bar{p}_T^4}{Q^3} \sinh(y - \eta) \left[M \cosh(y - \eta) - |\mathbf{q}_T| \cos\phi \right] ,
\end{aligned}
\tag{B.64}
$$

with $\bar{p}_T$ defined in Eq. (B.18). Now we compute the indefinte integral over $\cos\phi$. To do so, we need to use Eq. (B.19) along with the equality:

$$
\int \frac{dx}{(a \pm x)^3 \sqrt{1 - x^2}} = \frac{\sqrt{1 - x^2}\left[3ax \pm (4a^2 - 1) \right]}{2(a^2 - 1)^2 (x \pm a)^2} \pm \frac{(2a^2 + 1)}{(a^2 - 1)^{5/2}} \tan^{-1}\left(\frac{x \pm a(1 - \sqrt{1 - x^2})}{\sqrt{a^2 - 1}x} \right) .
\tag{B.65}
$$

This allows us to compute the integral([12]):

$$
\begin{aligned}
H(x,\eta) &= \left(\frac{4\pi Q^2}{3}\right)^{-1} \frac{\sinh(y-\eta)}{Q^3}\left[M\cosh(y-\eta)\int d(\phi)\,\overline{p}_T^4(\cos\phi) - |\mathbf{q}_T|\int d(\phi)\cos\phi\,\overline{p}_T^4(\cos\phi)\right] \\[2mm]
&= \frac{3Q^3\sinh(y-\eta)}{64\pi|\mathbf{q}_T|^4}\left[M\cosh(y-\eta)\int\frac{d(\phi)}{(a-\cos\phi)^4} - |\mathbf{q}_T|\int\frac{\cos\phi\,d(\phi)}{(a-\cos\phi)^4}\right] \\[2mm]
&= \frac{3Q^3\sinh(y-\eta)}{64\pi q_T^3}\int\frac{dx}{\sqrt{1-x^2}}\left[\frac{1}{(a-x)^3}+\frac{1}{(a+x)^3}\right] \\[2mm]
&= \frac{3Q^3\sinh(y-\eta)}{128\pi q_T^3}\left\{\frac{\sqrt{1-x^2}}{(a^2-1)^2}\left[\frac{2ax(3x^2-5a^2+2)}{(x^2-a^2)^2}\right]\right. \\[2mm]
&\quad + \left.\frac{2(2a^2+1)}{(a^2-1)^{5/2}}\left[\tan^{-1}\left(\frac{x\sqrt{E_q^2-q_T^2}}{\sqrt{1-x^2}E_q}\right)\right]\right\}
\end{aligned}
\tag{B.66}
$$

with $E_q = M\cosh(\eta-y)$, $q_T = |\mathbf{q}_T|$, and:

$$
a = \frac{E_q}{q_T}\,,
\tag{B.67}
$$

so that:

$$
\begin{aligned}
H(x,\eta) &= \frac{3Q^3\sinh(y-\eta)}{128\pi(E_q^2-q_T^2)^2}\left\{\frac{2x\sqrt{1-x^2}E_q q_T^2}{(x^2 q_T^2-E_q^2)^2}\left[3x^2 q_T^2+2q_T^2-5E_q^2\right]\right. \\[2mm]
&\quad + \left.\frac{2(2E_q^2+q_T^2)}{\sqrt{E_q^2-q_T^2}}\left[\tan^{-1}\left(\frac{x\sqrt{E_q^2-q_T^2}}{\sqrt{1-x^2}E_q}\right)\right]\right\}.
\end{aligned}
\tag{B.68}
$$

Finally, using the definition of H in Eq. (B.68), one can perform the integral over the fiducial phase space as discussed above in Eq. (B.35):

$$
\mathcal{P}_{\mathrm{PV}}(Q,y,q_T) = \int_{\eta_{\min}}^{\eta_{\max}} d\eta\,\vartheta(x_2(\eta)-x_1(\eta))\left[H(x_2(\eta),\eta)-H(x_1(\eta),\eta)\right].
\tag{B.69}
$$

This allows one to estimate the impact of the parity-violating contribution to the phase-space reduction factor.

In order to quantify numerically the impact of Eq. (B.69), Fig. B.3 displays the size $\mathcal{P}_{\mathrm{PV}}$ relative to the parity-conserving phase-space reduction factor as a function of y for three different values of q_T at $Q = M_Z$ and for the following lepton cuts: $p_{T,\ell} > 20$ GeV and $-2.4 < \eta_\ell < 2.4$. It turns out that the size of $\mathcal{P}_{\mathrm{PV}}$ relative to $\mathcal{P}$ is never larger than 2×10^{-6}. In addition, the rapid oscillations with y contribute to suppress even more the integral over realistic bins in y. One can thus conclude that, for realistic kinematic configurations, the impact of parity violating effects is completely negligible.

We finally notice that also following contraction enters the game in the presence of cuts on the leptonic final state:

$$
L_\phi = (z^\mu t^\nu + z^\nu t^\mu)L_{\mu\nu}\,.
\tag{B.70}
$$

We find that:

$$
L_\phi = 8(zp)\left[Q-2(tp)\right].
\tag{B.71}
$$

Using Eqs. (B.14) and (B.43), we have that:

$$
(zp) = p_T(\cosh\eta\sinh y - \sinh\eta\cosh y) = p_T\sinh(y-\eta)\,,
\tag{B.72}
$$

and:

$$
(tp) = \frac{1}{Q}\left[Mp_T\cosh(y-\eta) - \mathbf{q}_T\cdot\mathbf{p}_T\right] = \frac{p_T}{Q}\left[M\cosh(y-\eta) - q_T\cos\phi\right].
\tag{B.73}
$$

---

[12] The factor $\left(\frac{4\pi Q^2}{3}\right)^{-1}$ in Eq. (B.66) corresponds to the full phase-space in integral of $L_\perp$ in Eq. (B.54) that provides the natural normalisation.
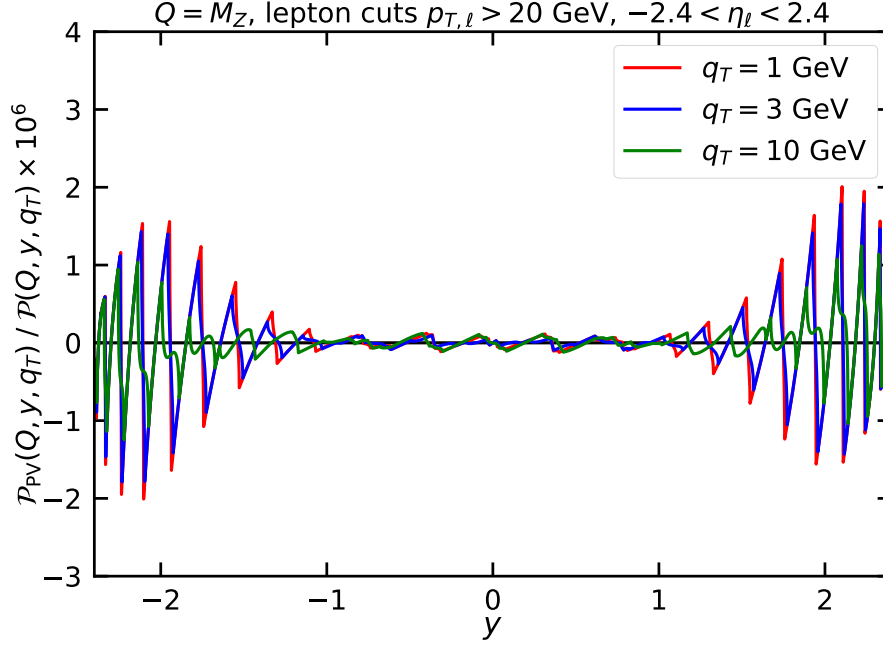
Fig. B.3: Ratio between the parity-violating phase-space reduction factor $\mathcal{P}_{\mathrm{PV}}$ in Eq. (B.69) and the respective parity-conserving factor as a function of the Z rapidity y at $Q = M_Z$ and for three different values of q_T, with lepton cuts equal to $p_{T,\ell} > 20$ GeV and $-2.4 < \eta_\ell < 2.4$.

Therefore:

$$L_\phi = 16 \frac{p_T^2}{Q} \sinh(y - \eta) \left[\frac{Q^2}{2p_T} - M \cosh(y - \eta) + q_T \cos\phi \right] = 16 \left[\frac{1}{2} p_T Q \sinh(y - \eta) - L_{\mathrm{PV}} \right]. \qquad \text{(B.74)}$$

Due to the presence of the overall factor $\sinh(y - \eta)$, also this contribution is expected to be subdominant.

B.3 Asymmetric cuts

In some circumstances, asymmetric cuts are necessary to match the experimental measurements. More specifically, the two outgoing leptons undergo different cuts depending on their hierarchy. Usually, one defines the (sub)leading lepton as the lepton with the (smallest) largest p_T and according to whether the lepton is leading or subleading a different cut on the p_T is enforced. In this case, the cut function Φ needs to be generalised as follows:

$$\Phi(p_1, p_2) = \vartheta(p_{T,1}^2 - p_{T,2}^2)\Theta^{(1)}(p_1)\Theta^{(2)}(p_2) + \vartheta(p_{T,2}^2 - p_{T,1}^2)\Theta^{(1)}(p_2)\Theta^{(2)}(p_1), \qquad \text{(B.75)}$$

where the functions $\Theta^{(1)}$ and $\Theta^{(2)}$ are defined as:

$$\Theta^{(i)}(p) = \vartheta(\eta - \eta_{\mathrm{min}})\vartheta(\eta_{\mathrm{max}} - \eta)\vartheta(p_T - p_{T,\mathrm{min}}^{(i)}), \quad i = 1, 2, \qquad \text{(B.76)}$$

with $p_{T,\mathrm{min}}^{(1)} \neq p_{T,\mathrm{min}}^{(2)}$ in general. As seen above, the lepton four-momenta p_1 and p_2 are subject to kinematic constraints such that one effectively has $p_1 = p$ and $p_2 = q - p$ with $p_{T,1} = \bar{p}_T$, with $\bar{p}_T$ defined in Eq. (B.18), and:

$$p_{T,2}^2 = q_T^2 + \bar{p}_T^2 - 2q_T\bar{p}_T \cos\phi. \qquad \text{(B.77)}$$

Therefore, the functions $\vartheta(p_{T,1}^2 - p_{T,2}^2)$ and $\vartheta(p_{T,2}^2 - p_{T,1}^2)$ can be reduced to the following ϑ-functions on the azimuthal angle ϕ:

$$\vartheta(p_{T,1}^2 - p_{T,2}^2) = \vartheta\left(\cos\phi - \frac{q_T \cosh(\eta - y)}{M}\right), \quad \vartheta(p_{T,2}^2 - p_{T,1}^2) = \vartheta\left(\frac{q_T \cosh(\eta - y)}{M} - \cos\phi\right). \qquad \text{(B.78)}$$

Generalising the procedure detailed above for the implementation of the cuts, one introduces the additional function:

$$f^{(1)}(\eta) = \frac{q_T \cosh(\eta - y)}{M} \, , \tag{B.79}$$

such that:

$$\Phi(p, q - p) = \vartheta(\eta - \eta_{\min})\vartheta(\eta_{\max} - \eta) \left[\vartheta(x - x_1^{(1)})\vartheta(x_2^{(1)} - x) + \vartheta(x - x_1^{(2)})\vartheta(x_2^{(2)} - x) \right] \, , \tag{B.80}$$

where we have defined:

$$
\begin{aligned}
x_1^{(1)}(\eta) &= \max[f^{(1)}(\eta), f^{(2)}(\eta, p_{T,\min}^{(1)}), -1] \, , \\[4pt]
x_2^{(1)}(\eta) &= \min[f^{(3)}(\eta, \eta_{\min}), f^{(3)}(\eta, \eta_{\max}), f^{(4)}(\eta, p_{T,\min}^{(2)}), 1] \, , \\[4pt]
x_1^{(2)}(\eta) &= \max[f^{(2)}(\eta, p_{T,\min}^{(2)}), -1] \, , \\[4pt]
x_2^{(2)}(\eta) &= \min[f^{(1)}(\eta), f^{(3)}(\eta, \eta_{\min}), f^{(3)}(\eta, \eta_{\max}), f^{(4)}(\eta, p_{T,\min}^{(1)}), 1] \, .
\end{aligned}
\tag{B.81}
$$

This gives:

$$
\begin{aligned}
\int_{-\infty}^{\infty} d\eta \int_{-1}^{1} dx \, \Phi(p, q - p) \ldots &= \int_{\eta_{\min}}^{\eta_{\max}} d\eta \left[\vartheta(x_2^{(1)}(\eta) - x_1^{(1)}(\eta)) \int_{x_1^{(1)}(\eta)}^{x_2^{(1)}(\eta)} dx \ldots \right. \\[6pt]
&\quad + \left. \vartheta(x_2^{(2)}(\eta) - x_1^{(2)}(\eta)) \int_{x_1^{(2)}(\eta)}^{x_2^{(2)}(\eta)} dx \ldots \right] .
\end{aligned}
\tag{B.82}
$$

Finally, one can exploit the ability to compute the primitive function of the integral in x to write the expression for the phase-space reduction factor for asymmetric cuts as follows:

$$
\begin{aligned}
\mathcal{P}(Q, y, q_T) &= \int_{\eta_{\min}}^{\eta_{\max}} d\eta \left\{ \vartheta(x_2^{(1)}(\eta) - x_1^{(1)}(\eta)) \left[\overline{F}(x_2^{(1)}(\eta), \eta) - \overline{F}(x_1^{(1)}(\eta), \eta) \right] \right. \\[6pt]
&\quad + \left. \vartheta(x_2^{(2)}(\eta) - x_1^{(2)}(\eta)) \left[\overline{F}(x_2^{(2)}(\eta), \eta) - \overline{F}(x_1^{(2)}(\eta), \eta) \right] \right\} ,
\end{aligned}
\tag{B.83}
$$

with $\overline{F}$ defined in Eq. (B.55). The same expression with $\overline{F}$ replaced by the function H given in Eq. (B.68) can be used for the parity-violating factor.

C   Differential cross section in the leptonic variables

The calculation of the phase-space reduction factor carried out in the previous section can be used to express the Drell-Yan cross section in Eq. (1.1) as differential in the kinematic variables of the single leptons. Loosely speaking, this amounts to removing the integral sign in the numerator in Eq. (B.1) but taking into account kinematic constraints. Using the transverse metric tensor $g_{\perp}^{\mu\nu}$, one finds:

$$d\mathcal{P} = \frac{d^4 p_1 d^4 p_2 \, \delta(p_1^2)\delta(p_2^2)\theta(p_{1,0})\theta(p_{2,0})\delta^{(4)}(p_1 + p_2 - q)L_\perp(p_1, p_2)}{\int d^4 p_1 d^4 p_2 \, \delta(p_1^2)\delta(p_2^2)\theta(p_{1,0})\theta(p_{2,0})\delta^{(4)}(p_1 + p_2 - q)L_\perp(p_1, p_2)} \, , \tag{C.1}$$

From Eq. (B.54), we know the value of the denominator. In the numerator, we can make use of the momentum-conservation and one of the on-shell-ness δ-functions. Using the r.h.s. of Eq. (B.45), but integrating over ϕ rather than $|\mathbf{p}_T|$, leads to:

$$\frac{d\mathcal{P}}{d|\mathbf{p}_T| d\eta} = \frac{3|\mathbf{p}_T|}{4\pi} \left[1 + 4\sinh^2(y - \eta)\frac{|\mathbf{p}_T|^2}{Q^2} \right] \int_0^{2\pi} d\phi \, \delta(Q^2 - 2|\mathbf{p}_T| \left[M \cosh(\eta - y) - |\mathbf{q}_T| \cos\phi \right]) \, , \tag{C.2}$$

where we have used Eqs. (B.8)-(B.12) and Eq. (B.16). Finally, to perform the integral over ϕ we use Eq. (B.19) to get:

$$\frac{d\mathcal{P}}{d|\mathbf{p}_T| d\eta} = \frac{3|\mathbf{p}_T|}{2\pi Q^2} \frac{Q^2 + 4|\mathbf{p}_T|^2 \sinh^2(\eta - y)}{\sqrt{4|\mathbf{p}_T|^2 |\mathbf{q}_T|^2 - (2|\mathbf{p}_T| M \cosh(\eta - y) - Q^2)^2}} \, . \tag{C.3}$$
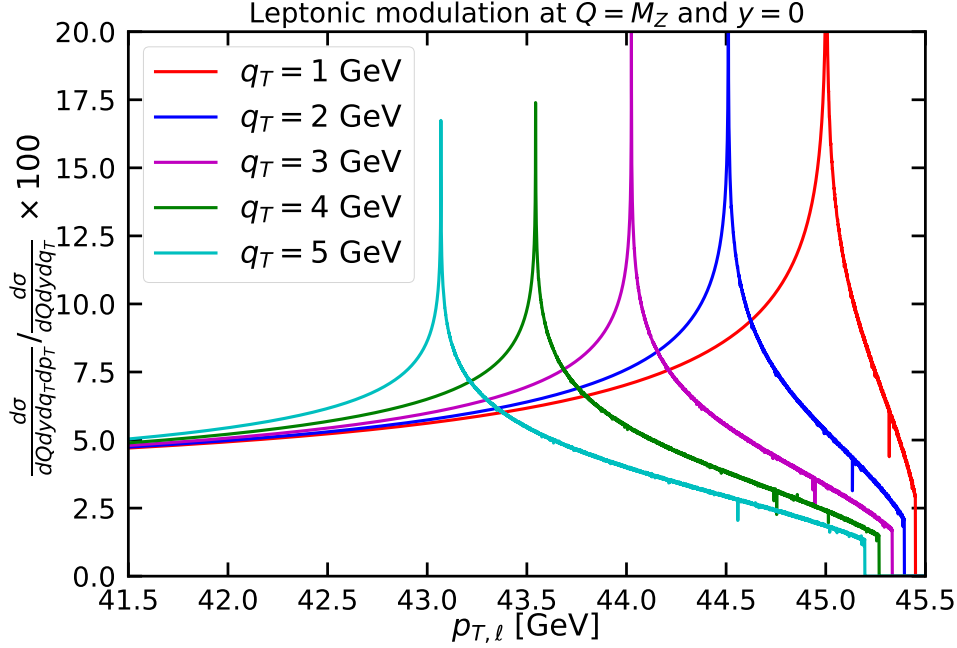
Fig. C.1: Behaviour of the second line of Eq. (C.7) at $Q = M_Z$ and $y = 0$ as a function of the lepton transverse momentum $p_{T,\ell}$.

Getting rid of the absolute value of the transverse vectors, this allows one to get the Drell-Yan cross section differential in the leptonic variables $|\mathbf{p}_T|$ and η:

$$\frac{d\sigma}{dQ\,dy\,dq_T\,d\eta\,dp_T} = \left[\frac{3p_T^2}{\pi Q^2 M} \frac{\left(\frac{Q^2}{4p_T^2} - 1\right) + \cosh^2(\eta - y)}{\sqrt{\frac{q_T^2}{M^2} - \left(\cosh(\eta - y) - \frac{Q^2}{2p_T M}\right)^2}} \right] \frac{d\sigma}{dQ\,dy\,dq_T} \ . \tag{C.4}$$

Due to the square root in the denominator, for fixed values of Q, q_T, and y, the expression above is defined for values of p_T and η such that:

$$\frac{Q^2}{2p_T M} - \frac{q_T}{M} < \cosh(\eta - y) < \frac{Q^2}{2p_T M} + \frac{q_T}{M} \ . \tag{C.5}$$

In order to focus on the p_T dependence of the cross section, one may want to integrate of the lepton rapidity η. Using the analogous of Eq. (B.19) for $\cosh(\eta)$:

$$\int_{-\infty}^{\infty} d\eta\, f(\cos\eta) = \int_{1}^{\infty} \frac{dx}{\sqrt{x^2 - 1}} \left[f(x) + f(-x) \right] \ , \tag{C.6}$$

and taking into account the constraint in Eq. (C.5), one finds:

$$\frac{d\sigma}{dQ\,dy\,dq_T\,dp_T} = \frac{d\sigma}{dQ\,dy\,dq_T} \times$$

$$\frac{3p_T}{2\pi Q^2} \int_{-\frac{q_T}{M}}^{\frac{q_T}{M}} \frac{dx}{\sqrt{\frac{q_T^2}{M^2} - x^2}} \left(\frac{\left(\frac{Q^2}{4p_T^2} - 1\right) + \left(x + \frac{Q^2}{2p_T M}\right)^2}{\sqrt{\left(x + \frac{Q^2}{2p_T M}\right)^2 - 1}} + \frac{\left(\frac{Q^2}{4p_T^2} - 1\right) + \left(x - \frac{Q^2}{2p_T M}\right)^2}{\sqrt{\left(x - \frac{Q^2}{2p_T M}\right)^2 - 1}} \right) \ . \tag{C.7}$$

For fixed values of Q, q_T, and y, the integral above can be solved numerically and plotted as a function of p_T. The result is shown in Fig. C.1.

D   Convolution in transverse-momentum space

The "transverse-momentum" version of Eq. (1.1) reads:

$$
\frac{d\sigma}{dQdydq_T} = \frac{16\pi\alpha^2 q_T}{9Q^3} H(Q,\mu) \sum_q C_q(Q)
$$

$$
\times \int d^2\mathbf{k}_{T,1} d^2\mathbf{k}_{T,2} \overline{F}_q(x_1, \mathbf{k}_{T,1}; \mu, \zeta) \overline{F}_{\bar{q}}(x_2, \mathbf{k}_{T,2}; \mu, \zeta) \delta^{(2)}(\mathbf{q}_T - \mathbf{k}_{T,1} - \mathbf{k}_{T,2}),
$$

(D.1)

where, with abuse of notation, we used the same symbol for the distributions F both in k_T and b_T space. We can make use of the δ-function to reduce the expression above to:

$$
\frac{d\sigma}{dQdydq_T} = \frac{16\pi\alpha^2 q_T}{9Q^3} H(Q,\mu) \sum_q C_q(Q) \int d^2\mathbf{k}_T \overline{F}_q(x_1, \mathbf{k}_T; \mu, \zeta) \overline{F}_{\bar{q}}(x_2, \mathbf{q}_T - \mathbf{k}_T; \mu, \zeta). \tag{D.2}
$$

Since the distributions F only depend on the absolute value of their argument (be it k_T or b_T), the expression above can be further reduced to:

$$
\frac{d\sigma}{dQdydq_T} = \frac{16\pi\alpha^2 q_T}{9Q^3} H(Q,\mu) \sum_q C_q(Q)
$$

$$
\times \int_0^\infty dk_T\, k_T \int_0^{2\pi} d\theta\, \overline{F}_q(x_1, k_T; \mu, \zeta) \overline{F}_{\bar{q}}(x_2, \sqrt{q_T^2 + k_T^2 - 2q_T k_T \cos\theta}; \mu, \zeta),
$$

(D.3)

where, without loss of generality, we are assuming that the vector $\mathbf{q}_T$ is directed along the x axis. Knowing the functions F in k_T space, the formula above can be implemented numerically.

E   The A_0 coefficient

Using Eq. (5) of Ref. [6], the azimuthal angle θ of the (negative) lepton in the Collins-Soper frame can be related to the momenta on the vector boson and of one of the leptons in the laboratory frame as:

$$
\cos\theta(\eta, p_T) = \mathrm{sign}(y)\frac{2p_T}{Q}\sinh(y - \eta). \tag{E.1}
$$

This can be related to the coefficient A_0 as [7]:

$$
A_0 = 4 - 10 \left\langle \cos^2\theta \right\rangle, \tag{E.2}
$$

where:

$$
\left\langle \cos^2\theta \right\rangle \equiv \left[\int dp_T d\eta \frac{d\sigma}{dQdydq_T d\eta dp_T} \right]^{-1} \int dp_T d\eta \left[\cos\theta(\eta, p_T) \right]^2 \frac{d\sigma}{dQdydq_T d\eta dp_T}. \tag{E.3}
$$

If the integration in both numerator and denominator in the r.h.s. of the quantity above is performed over the full phase space, the result at small q_T is:

$$
\left\langle \cos^2\theta \right\rangle = \int dp_T d\eta \left[\cos\theta(\eta, p_T) \right]^2 \frac{d\mathcal{P}}{dp_T d\eta} \tag{E.4}
$$

with the element of phase space $d\mathcal{P}$ is given in Eq. (C.3). Therefore, the "QCD dynamics" totally cancels in the ratio and one is left with a relatively interesting kinematic factor.

F   Implementing the $\phi*$ distribution

A physical observable that is particularly useful to probe the intrinsic transverse dynamics of hadrons is the so-called ϕ^* distribution in Drell-Yan production, defined as [8]:

$$
\phi^* = \tan\left(\frac{\pi - \Delta\phi}{2}\right)\sin\theta^* = \tan\left(\frac{\pi - \Delta\phi}{2}\right)\sqrt{1 - \tanh^2\left(\frac{\Delta\eta}{2}\right)}, \tag{F.1}
$$

where $\Delta\phi = \phi_1 - \phi_2$ and $\Delta\eta = \eta_1 - \eta_2$ are the separation in azimuthal angle and pseudo-rapidity of the two outgoing leptons. The reason why ϕ^* is interesting is that experimental measurements of this quantity reach an extremely high accuracy. It is therefore useful to express the Drell-Yan cross section differential in q_T into a cross section differential in ϕ^*. This is achieved through the chain rule:

$$\frac{d\sigma}{dQ\,dy\,dq_T\,d\eta\,dp_T} = \frac{d\phi^*}{dq_T}\frac{d\sigma}{dQ\,dy\,d\phi^*\,d\eta\,dp_T}\,. \tag{F.2}$$

Of course, this requires the knowledge of ϕ^* as a function of q_T which is what we will work out in the following. The starting point is the four-momentum conservation $q = p_1 + p_2$. Taking the absolute value of this relation and using the parameterisations in Eq. (B.13) for q and in Eq. (B.14) for both p_1 and p_2 immediately gives:

$$\cosh\Delta\eta = 1 + \frac{Q^2}{2p_{T1}p_{T2}}\,. \tag{F.3}$$

In addition, equating the absolute values of the transverse component ($|\mathbf{q}_T|^2 = |\mathbf{p}_{T1} + \mathbf{p}_{T2}|^2$) leads to:

$$\cos\Delta\phi = \frac{p_{T1}^2 + p_{T2}^2 - q_T^2}{2p_{T1}p_{T2}}\,. \tag{F.4}$$

Using Eq. (F.3) one has:

$$\tanh\left(\frac{\Delta\eta}{2}\right) = \sqrt{\frac{\cosh\Delta\eta - 1}{\cosh\Delta\eta + 1}} = \sqrt{\frac{Q^2}{Q^2 + 4p_{T1}p_{T2}}}\,, \tag{F.5}$$

so that:

$$\sin\theta^* = \sqrt{1 - \tanh^2\left(\frac{\Delta\eta}{2}\right)} = \sqrt{\frac{4p_{T1}p_{T2}}{Q^2 + 4p_{T1}p_{T2}}}\,. \tag{F.6}$$

On the other hand, using Eq. (F.4) one finds:

$$\tan\left(\frac{\pi - \Delta\phi}{2}\right) = \sqrt{\frac{1 - \cos(\pi - \Delta\phi)}{1 + \cos(\pi - \Delta\phi)}} = \sqrt{\frac{1 + \cos\Delta\phi}{1 - \cos\Delta\phi}} = \sqrt{\frac{p_{T1}^2 + p_{T2}^2 - q_T^2 + 2p_{T1}p_{T2}}{p_{T1}^2 + p_{T2}^2 - q_T^2 - 2p_{T1}p_{T2}}}\,. \tag{F.7}$$

Now let us define $p_{T1} = p_T$ and $\eta = \eta_1$ and trade p_{T2} for $\cosh(y - \eta)$ using the relation:

$$p_{T2}^2 = M^2 + p_T^2 - 2p_T M \cosh(y - \eta) \tag{F.8}$$

with $M = \sqrt{Q^2 + q_T^2}$. This gives:

$$\sin\theta^* = \sqrt{\frac{4p_T\sqrt{M^2 + p_T^2 - 2p_T M \cosh(y - \eta)}}{Q^2 + 4p_T\sqrt{M^2 + p_T^2 - 2p_T M \cosh(y - \eta)}}}\,. \tag{F.9}$$

and:

$$\tan\left(\frac{\pi - \Delta\phi}{2}\right) = \sqrt{\frac{Q^2 + 2p_T\left[p_T - M\cosh(y - \eta) + \sqrt{M^2 + p_T^2 - 2p_T M \cosh(y - \eta)}\right]}{Q^2 + 2p_T\left[p_T - M\cosh(y - \eta) - \sqrt{M^2 + p_T^2 - 2p_T M \cosh(y - \eta)}\right]}}\,. \tag{F.10}$$

Gathering all pieces together finally gives:

$$\begin{aligned}
\phi^* &= \sqrt{\frac{Q^2 + 2p_T\left[p_T - M\cosh(y - \eta) + \sqrt{M^2 + p_T^2 - 2p_T M \cosh(y - \eta)}\right]}{Q^2 + 2p_T\left[p_T - M\cosh(y - \eta) - \sqrt{M^2 + p_T^2 - 2p_T M \cosh(y - \eta)}\right]}} \\
&\times \sqrt{\frac{4p_T\sqrt{M^2 + p_T^2 - 2p_T M \cosh(y - \eta)}}{Q^2 + 4p_T\sqrt{M^2 + p_T^2 - 2p_T M \cosh(y - \eta)}}}\,.
\end{aligned} \tag{F.11}$$

One can show that the boost required to go from the laboratory frame, in which the vectors q and p are given by Eqs. (B.13) and (B.14), respectively, with p_T given by Eq. (B.18), to the Collins-Soper frame, in which:

$$q = Q(1, 0, 0, 0) \quad \text{and} \quad p = \frac{Q}{2}(1, \sin\theta\cos\phi, \sin\theta\sin\phi, \cos\theta)\,, \tag{F.12}$$

is given by:

$$\Lambda_{\text{Lab}\to\text{CS}} = \begin{pmatrix} \frac{M}{Q}\cosh y & -\frac{q_T}{Q} & 0 & -\frac{M}{Q}\sinh y \\ -\frac{q_T}{Q}\cosh y & \frac{M}{Q} & 0 & \frac{q_T}{Q}\sinh y \\ 0 & 0 & 1 & 0 \\ -\sinh y & 0 & 0 & \cosh y \end{pmatrix}, \tag{F.13}$$

with $M = \sqrt{Q^2 + q_T^2}$. Likewise, the boost to go from the Collins-Soper to the laboratory frame is the inverse of the above transformation and reads:

$$\Lambda_{\text{CS}\to\text{Lab}} = \Lambda_{\text{Lab}\to\text{CS}}^{-1} = \begin{pmatrix} \frac{M}{Q}\cosh y & \frac{q_T}{Q}\cosh y & 0 & \sinh y \\ \frac{q_T}{Q} & \frac{M}{Q} & 0 & 0 \\ 0 & 0 & 1 & 0 \\ \frac{M}{Q}\sinh y & \frac{q_T}{Q}\sinh y & 0 & \cosh y \end{pmatrix}. \tag{F.14}$$

Notice that rotating the vector in Eq. (B.14) using the transformation in Eq. (F.13) and equating the z component to that of the vector p in Eq. (F.12) immediately gives Eq. (E.1). This immediately allows one to write:

$$\sin\theta = \frac{\sqrt{Q^2 - 4p_T\sinh^2(\eta - y)}}{Q} \tag{F.15}$$

G   QED radiative corrections to the leptonic final state

In this section, we will show how to include into the Drell-Yan cross section the corrections due to QED final-state collinear radiation. This will be done at LO + (N)LL accuracy which means that the leptonic tensor will be computed at the first fixed perturbative order while the collinear radiation will be resummed to the first (second) logarithmic order.

Assuming massless, unpolarised leptons, considering only collinear radiation, and concentrating on cross sections integrated over the polar angle, the leptonic tensor can be generally decomposed into the following Lorentz structures [9]:

$$\begin{aligned} L^{\mu\nu}(q, p_1, p_2) &= \left(-g^{\mu\nu} + \frac{q^\mu q^\nu}{Q^2}\right)\mathcal{F}_1(z_1, z_2, Q^2) + \frac{1}{p\cdot q}\left(p^\mu - \frac{p\cdot q}{Q^2}q^\mu\right)\left(p^\nu - \frac{p\cdot q}{Q^2}q^\nu\right)\mathcal{F}_2(z_1, z_2, Q^2) \\ &\quad - i\varepsilon^{\mu\nu\rho\sigma}\frac{q_\rho p_\sigma}{2p\cdot q}\mathcal{F}_3(z_1, z_2, Q^2). \end{aligned} \tag{G.1}$$

where $p = p_1$, $Q^2 = q^2$, $z_i = 2p_i\cdot q/Q^2$ with $i = 1, 2$, and where the functions $\mathcal{F}$ are purposely reminiscent of the semi-inclusive DIS structure functions. This structure functions allow a collinear factorisation in terms of hard cross sections and collinear fragmentation functions (FFs):

$$\mathcal{F}_S(z_1, z_2, Q^2) = c_S(Q^2)\sum_{i,j=e^\pm,\gamma}\int_{z_1}^1\frac{dy_1}{y_1}\int_{z_2}^1\frac{dy_2}{y_2}C_{ij}^{(S)}\left(\frac{y_1}{z_1}, \frac{y_2}{z_2}, \alpha(Q)\right)d_{i/e^-}(y_1, Q)d_{j/e^+}(y_2, Q), \quad S = 1, 2, 3, \tag{G.2}$$

where c_S is the appropriate electroweak charge (that also contains the vector-boson propagator) with $c_1 = c_2$. Therefore, the fully differential cross section for inclusive Drell-Yan production in hadronic collisions reads:

$$\frac{d\sigma}{d^4p_1 d^4p_2} = \int d^4q\, W_{\mu\nu}(P_1, P_2, q)L^{\mu\nu}(q, p_1, p_2), \tag{G.3}$$

where $W_{\mu\nu}$ is the hadronic tensor and $P_{1,2}$ are the momenta of the incoming hadrons. Notice that here we are assuming that there is non interference between in the leptonic and the hadronic parts. Importantly, one generally has $q \neq p_1 + p_2$ due to possible radiation that is eventually integrated over into the structure functions. The differential cross section with respect to the lepton-pair momentum $\bar{q} = p_1 + p_2$ within a certain fiducial region defined by the function $\Theta(p_1, p_2)$ is computed as:

$$\frac{d\sigma}{d^4\bar{q}} = \int d^4p_1 d^4p_2\left[\int d^4q\, W_{\mu\nu}(P_1, P_2, q)L^{\mu\nu}(q, p_1, p_2)\right]\delta^{(4)}(\bar{q} - p_1 - p_2)\Theta(p_1, p_2). \tag{G.4}$$

If no QED radiation, either hard or collinear, is allowed the hard cross sections reduce to:

$$C^{(S)}_{ij,\text{LO}}(y_1, y_2, \alpha(Q)) = \delta_{ie^-}\delta_{je^+}\delta(1 - y_1)\delta(1 - y_2).$$ (G.5)

and the relevant FFs to:

$$d_{e^\pm/e^\pm}(y, Q) = \delta(1 - y).$$ (G.6)

such that the structure functions are all equal and become:

$$\mathcal{F}_{S,\text{LO}}(z_1, z_2, Q^2) = \delta(1 - z_1)\delta(1 - z_2) = Q^4\delta(p_2^2)\delta(p_1^2)\theta(p_{1,0})\theta(p_{2,0}).$$ (G.7)

Plugging this identity into the leptonic tensor and requiring $q = p_1 + p_2$ (see below), one finds:

$$L^{\mu\nu}(p_1 + p_2, p_1, p_2) = Q^2\left[2c_1\left(-g^{\mu\nu}p_1 \cdot p_2 + p_1^\mu p_2^\nu + p_2^\mu p_1^\nu\right) + ic_3\varepsilon^{\mu\nu\rho\sigma}p_{1\rho}p_{2\sigma}\right]\delta(p_1^2)\delta(p_2^2)\theta(p_{1,0})\theta(p_{2,0}),$$ (G.8)

that is the well-known leptonic tensor multiplied by the on-shell-ness condition for the leptons. Now the cross section differential in $q = p_1 + p_2$ within a specific set of fiducial cuts on the outgoing leptons defined by the function $\Theta(p_1, p_2)$ is computed as:

$$\frac{d\sigma}{d^4q} = \int d^4p_1 d^4p_2 W_{\mu\nu}(P_1, P_2, q)L^{\mu\nu}(q, p_1, p_2)\delta^{(4)}(q - p_1 - p_2)\Theta(p_1, p_2),$$ (G.9)

where $W_{\mu\nu}$ is the hadronic tensor. Decomposing the hadronic tensor in terms of Lorentz structures and taking the contractions with the leptonic tensor produces the fiducial cross section discussed above. The Lorentz structure relevant to the unpolaised case is $g_\perp^{\mu\nu}$ given in Eq. (B.42). Observing the fact that $g_\perp^{\mu\nu}$ is symmetric, when contracting it with the leptonic tensor in Eq. (G.1), the term proportional to $\epsilon^{\mu\nu\rho\sigma}$ automatically drops. We are then left with:

$$L_\perp(q, p_1, p_2) = g_\perp^{\mu\nu}L_{\mu\nu}(q, p_1, p_2) = -2\mathcal{F}_1(z_1, z_2, Q^2) - \frac{1}{2}z_1\mathcal{F}_2(z_1, z_2, Q^2) + \frac{(zp)^2}{p \cdot q}\mathcal{F}_2(z_1, z_2, Q^2)$$ (G.10)

where we have used the equalities $z^2 = -1$, $t^2 = 1$, $zq = 0$, and $p^2 = 0$.

References

[1] I. Scimemi and A. Vladimirov, "Analysis of vector boson production within TMD factorization," *Eur. Phys. J. C*, vol. 78, no. 2, p. 89, 2018.

[2] J. Collins, *Foundations of perturbative QCD*, vol. 32. Cambridge University Press, 11 2013.

[3] H. Ogata, "A numerical integration formula based on the bessel functions,"

[4] P. L. McGaughey *et al.*, "Cross-sections for the production of high mass muon pairs from 800-GeV proton bombardment of H-2," *Phys. Rev. D*, vol. 50, pp. 3038–3045, 1994. [Erratum: Phys.Rev.D 60, 119903 (1999)].

[5] A. Bacchetta, F. Delcarro, C. Pisano, M. Radici, and A. Signori, "Extraction of partonic transverse momentum distributions from semi-inclusive deep-inelastic scattering, Drell-Yan and Z-boson production," *JHEP*, vol. 06, p. 081, 2017. [Erratum: JHEP 06, 051 (2019)].

[6] E. Richter-Was and Z. Was, "Separating electroweak and strong interactions in Drell–Yan processes at LHC: leptons angular distributions and reference frames," *Eur. Phys. J. C*, vol. 76, no. 8, p. 473, 2016.

[7] R. Gauld, A. Gehrmann-De Ridder, T. Gehrmann, E. Glover, and A. Huss, "Precise predictions for the angular coefficients in Z-boson production at the LHC," *JHEP*, vol. 11, p. 003, 2017.

[8] A. Banfi, S. Redford, M. Vesterinen, P. Waller, and T. Wyatt, "Optimisation of variables for studying dilepton transverse momentum distributions at hadron colliders," *Eur. Phys. J. C*, vol. 71, p. 1600, 2011.

[9] M. A. Ebert, J. K. L. Michel, I. W. Stewart, and F. J. Tackmann, "Drell-Yan q_T resummation of fiducial power corrections at N^{3}LL," *JHEP*, vol. 04, p. 102, 2021.